



NATIONAL ENERGY TECHNOLOGY LABORATORY

# Thermodynamic Properties of CO<sub>2</sub> Capture Reaction by Solid Sorbents: Theoretical Predictions and Experimental Validations

Yuhua Duan<sup>1</sup>, David Luebke<sup>1</sup>, Henry Pennline<sup>1</sup>  
Liyu Li<sup>2</sup>, David King<sup>2</sup>, Keling Zhang<sup>2</sup>, Lifeng Zhao<sup>3</sup>, Yunhan Xiao<sup>3</sup>

<sup>1</sup>DOE-National Energy Technology Lab. Pittsburgh, PA 15236

<sup>2</sup>Institute for Interfacial Catalysis, Pacific Northwest National Laboratory, Richland, WA 99354

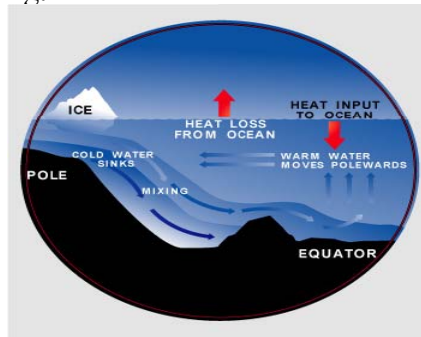
<sup>3</sup>Institute of Engineering Thermodynamics, Chinese Academy of Sciences, Beijing 100190, P. R. China

2012 International Pittsburgh Coal Conference  
(Oct. 17, 2012, Pittsburgh, PA)



## Motivation

- CO<sub>2</sub> emission causes Global Warming.



- Current CO<sub>2</sub> sorbents have big limitations due to large energy usage → high operating costs.
- Need to identify good CO<sub>2</sub> sorbents with optimal energy usage.
- Theoretical simulations are powerful tools for selecting good candidates of CO<sub>2</sub> sorbents.

2

NATIONAL ENERGY TECHNOLOGY LABORATORY

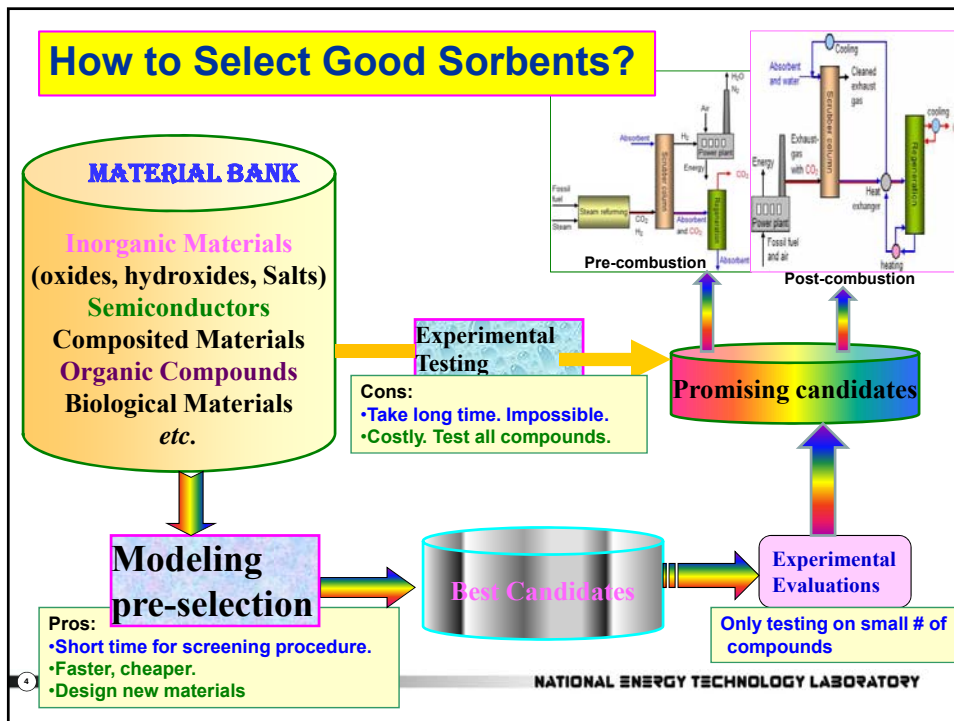
## Objectives

- We are establishing *a theoretical procedure* to identify most potential candidates of CO<sub>2</sub> solid sorbents from a large solid material databank to meet the **DOE programmatic goal** for energy conversion;
- To explore the optimal working conditions for the promising CO<sub>2</sub> solid sorbents, especially from room to warm T ranges with optimal energy usage, used for both pre- and post-combustion capture technologies.

3

NATIONAL ENERGY TECHNOLOGY LABORATORY

## How to Select Good Sorbents?



3

NATIONAL ENERGY TECHNOLOGY LABORATORY

## Our Modeling Approach (1)

•For reaction,  $\text{Solid}_A + \text{CO}_2 + [\text{H}_2\text{O}] \leftrightarrow \text{Solid}_B + [\text{solid}_C] + [\text{H}_2\text{O}]$ ,  
 where [...] is optional, the chemical potential is:

$$\Delta\mu(T, P) = \Delta\mu^0(T) - RT \ln \frac{P_{\text{CO}_2}}{P_{\text{H}_2\text{O}}^{\pm 1}}$$

If no H<sub>2</sub>O involved, P<sub>H<sub>2</sub>O</sub> term vanished

•Search literature and known database. If the thermodynamic properties of all solids involved are known,

$$\Delta\mu^0(T) \approx \Delta G_{\text{product}}^{\text{solid}}(T) - \Delta G_{\text{reactant}}^{\text{solid}}(T) - G_{\text{CO}_2}(T) \pm G_{\text{H}_2\text{O}}(T)$$

•Reaction Heat:

$$\Delta H(T) = \Delta H_{\text{product}}^{\text{solid}}(T) - \Delta H_{\text{reactant}}^{\text{solid}}(T) - \Delta H_{\text{CO}_2}(T) \pm \Delta H_{\text{H}_2\text{O}}(T)$$

- Y. Duan, *Proc. of 7<sup>th</sup> Ann. Conf. on Carbon Capture & Sequestration*, 2008
- Y. Duan, *Phys. Rev. B* 77(2008)045332
- Y. Duan & D. C. Sorescu, *Phys. Rev. B* 79(2009)014301, *J. Chem. Phys.* 133(2010)074508
- Y. Duan, D. Luebke, H. Pennline, *Int. J. Clean Coal & Energy*, 1(2012)1-11

## Our Theoretical Approach (2)

•For reaction,  $\text{Solid}_A + \text{CO}_2 + [\text{H}_2\text{O}] \leftrightarrow \text{Solid}_B + [\text{solid}_C] + [\text{H}_2\text{O}]$ ,  
 where [...] is optional, the chemical potential is:

If the thermodynamic data of solids are not available

$$\Delta\mu(T, P) = \Delta\mu^0(T) - RT \ln \frac{P_{\text{CO}_2}}{P_{\text{H}_2\text{O}}^{\pm 1}}$$

where

$$\Delta\mu^0(T) \approx \Delta E^{\text{DFT}} - G_{\text{CO}_2}(T) \pm G_{\text{H}_2\text{O}}(T) + \Delta E_{\text{ZP}} + \Delta F^{\text{PH}}(T)$$

VASP

Ideal gas  
Statistics physics

For solids  
Phonon dynamics

First approximation:  
do DFT calculation only

Filter I

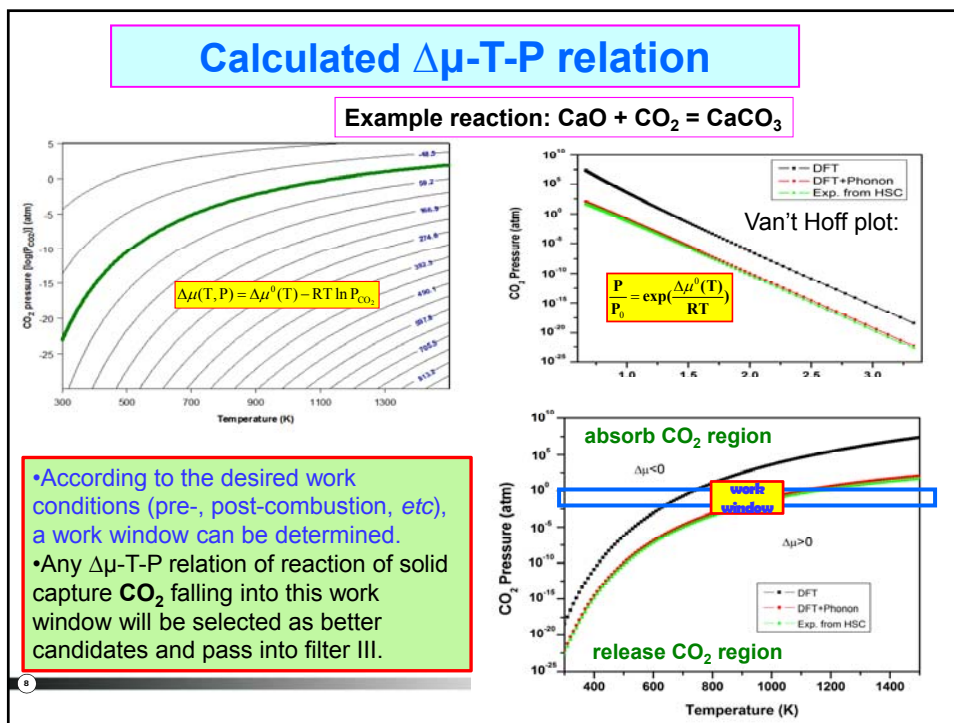
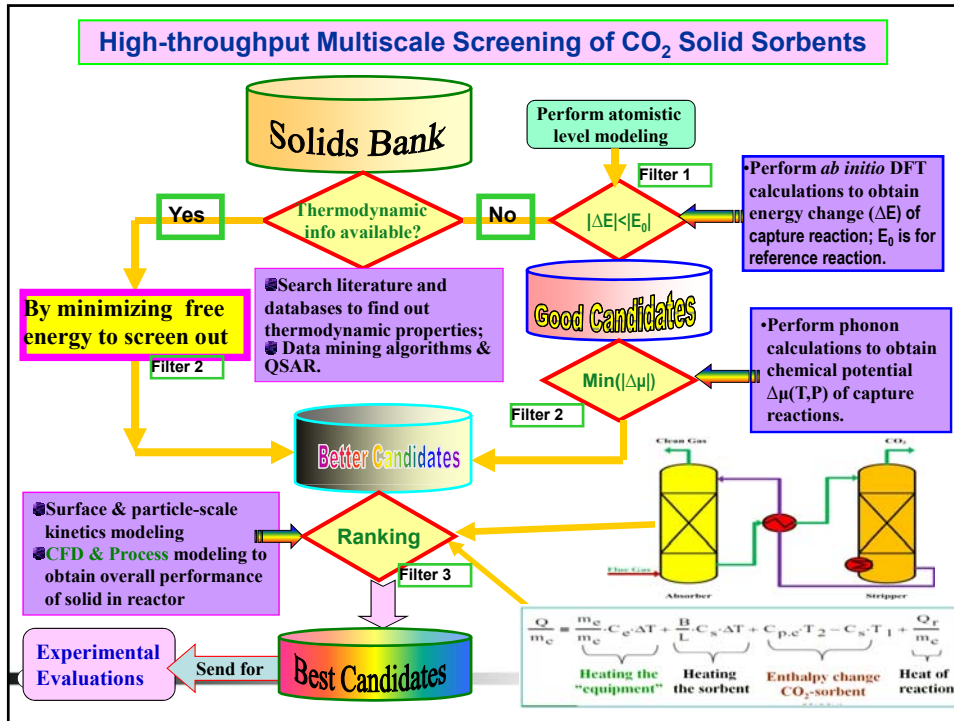
Filter II

For these promised candidate selected by filter I based on a reference capture reaction, do phonon free energy and entropy calculations.

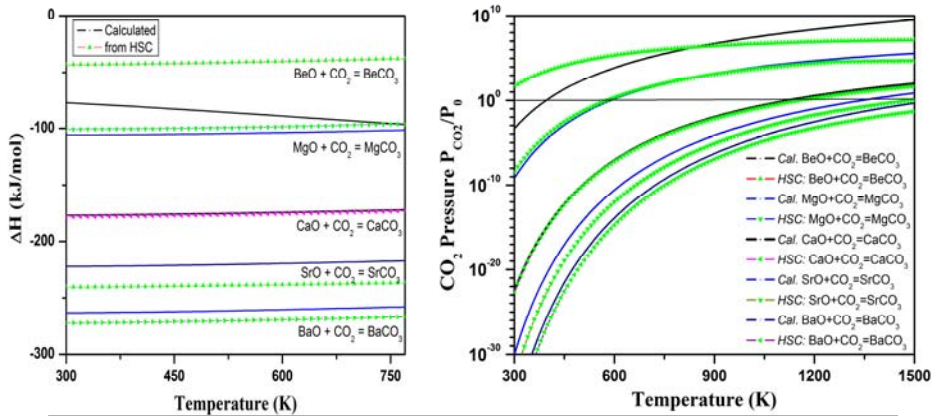
Reaction Heat:

$$\Delta H^{\text{cal}}(T) = \Delta\mu^0(T) + T * (-S_{\text{CO}_2} \pm S_{\text{H}_2\text{O}} + \Delta S_{\text{harm}})$$

- Y. Duan, *Proc. of 7<sup>th</sup> Ann. Conf. on Carbon Capture & Sequestration*, 2008
- Y. Duan & D. C. Sorescu, *Phys. Rev. B* 79(2009)014301, *J. Chem. Phys.* 133(2010)074508
- Y. Duan, D. Luebke, H. Pennline, *Int. J. Clean Coal & Energy*, 1(2012)1-11



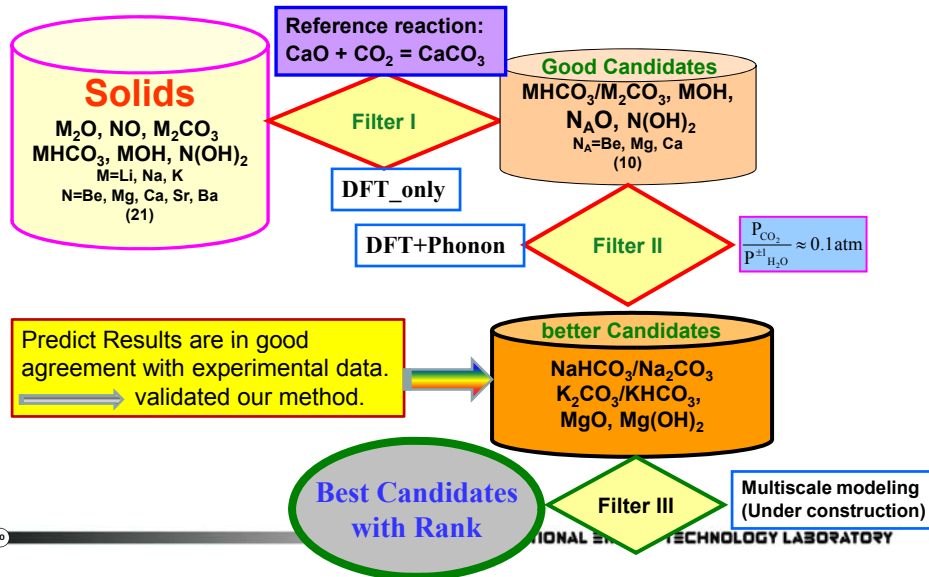
## Calculated Results of Alkaline Oxides

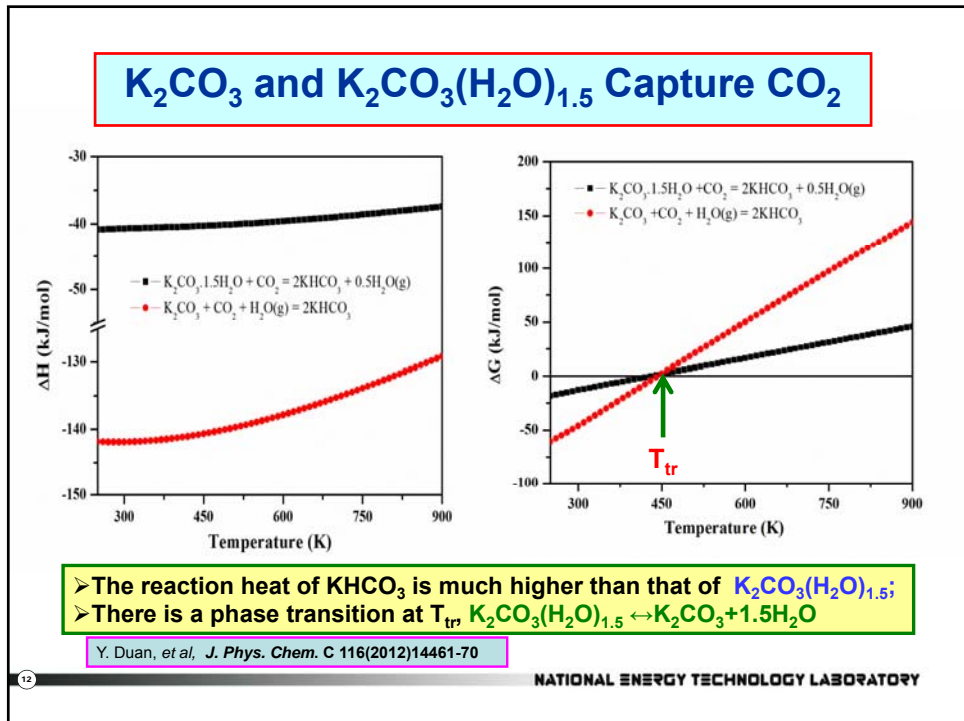
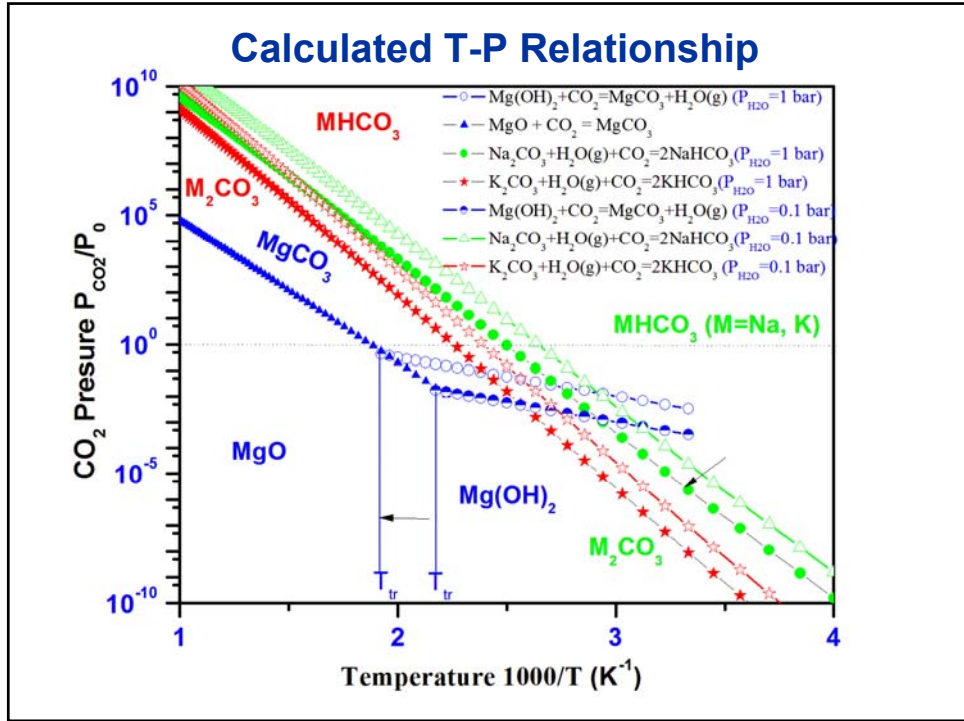


From them, at given capture conditions (T,P), the suitable sorbents can be identified.  
 Except for BeO and Be(OH)<sub>2</sub> systems, our DFT+Phonon calculated results are in good agreement with experimental measurements.

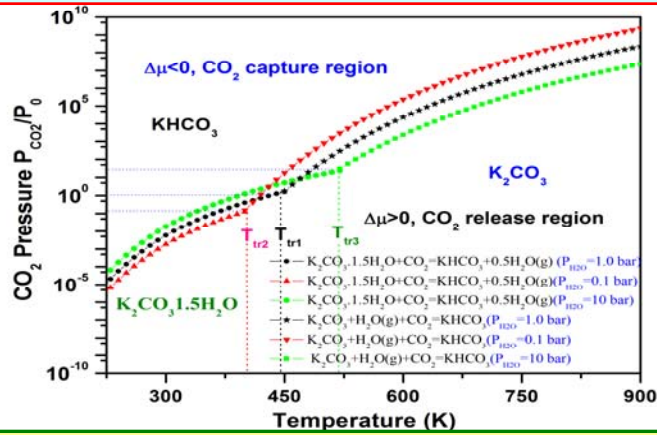
- Y. Duan, D. C. Sorescu, *J. Chem. Phys.* 133(2010)074508
- Y. Duan, B. Zhang, D.C. Sorescu, J. K. Johnson, *J. Solid State Chem.* 184(2011)403-311
- B. Zhang, Y. Duan, J. K. Johnson, *J. Chem. Phys.* 136(2012)064516
- Y. Duan, B. Zhang, D.C. Sorescu, J. K. Johnson, et al. *J. Phys. Condens Matter* 24(2012)325501

## In the Case of Alkali & Alkaline Metal Oxides, Hydroxides, Bicarbonates





## Phase-diagram of $K_2CO_3$ - $CO_2$ - $H_2O$



The regenerated solid from  $KHCO_3$  depends on the  $P_{H_2O}$  and  $T$ :

- With high  $P_{H_2O}$ , at low temperature ( $<T_{tr}$ ), get  $K_2CO_3(H_2O)_{1.5}$ ;
- Above  $T_{tr}$ , obtain anhydrous  $K_2CO_3$ ;
- $T_{tr}$  can be increased by increasing  $P_{H_2O}$ .

Y. Duan, et al, J. Phys. Chem. C 116(2012)14461-70

NATIONAL ENERGY TECHNOLOGY LABORATORY

The calculated thermodynamic properties of reactions of  $CO_2$  captured by anhydrous and dehydrated potassium carbonates.  $T_1$  refers Pre-combustion while  $T_2$  refers Post-combustion.

Reactions	$CO_2$ wt%	$\Delta E_{DFT}$ (kJ/mol)	$\Delta E_{ZP}$ (kJ/mol)	$\Delta H$ ( $T=300K$ ) (kJ/mol)	$\Delta G$ ( $T=300K$ ) (kJ/mol)	$T_1$ (K)	$T_2$ (K)	$T_{tr}$ (K)
$K_2CO_3 \cdot 1.5H_2O + CO_2 = 2KHCO_3 + 0.5H_2O(g)$	26.88	-40.47	-0.74	-40.68	-12.82	580 <sup>b</sup> 665 <sup>c</sup> 510 <sup>d</sup>	370 <sup>b</sup> 395 <sup>c</sup> 335 <sup>d</sup>	445 <sup>b</sup> 395 <sup>c</sup> 515 <sup>d</sup>
$K_2CO_3 + CO_2 + H_2O(g) = 2KHCO_3$	31.84	-154.43	18.29	-141.73 -142.85 <sup>a</sup>	-46.28 -44.72 <sup>a</sup>	490 <sup>b</sup> 455 <sup>c</sup> 515 <sup>d</sup>	420 <sup>b</sup> 395 <sup>c</sup> 445 <sup>d</sup>	

<sup>a</sup> Calculated by Chemistry package<sup>16</sup>

<sup>b</sup> when  $P_{H_2O} = 1$  bar

<sup>c</sup> when  $P_{H_2O} = 0.1$  bar

<sup>d</sup> when  $P_{H_2O} = 10$  bar

NATIONAL ENERGY TECHNOLOGY LABORATORY

## Characterization of MgO-Na<sub>2</sub>CO<sub>3</sub> warm CO<sub>2</sub> absorbent

**Session #21:** Xiaohong Li *et al*, "Mg-CaCO<sub>3</sub> double salt absorbents for CO<sub>2</sub> removal at 300-500°C", Tuesday, 17:05.

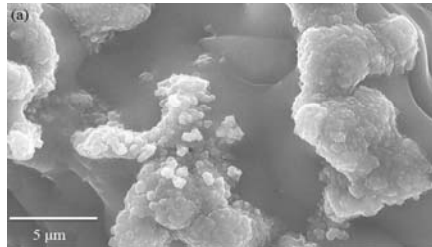
**Session #29:** Keling Zhang *et al*, "Carbon capture –promoted syngas utilization for production of fuels and chemicals", Wednesday, 14:50

15

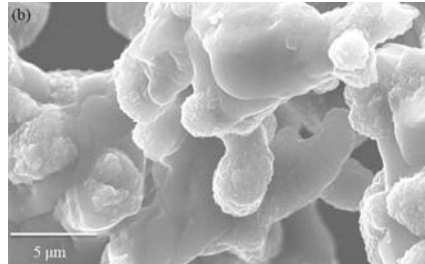
NATIONAL ENERGY TECHNOLOGY LABORATORY

## Characterization of MgO-Na<sub>2</sub>CO<sub>3</sub> warm CO<sub>2</sub> absorbent

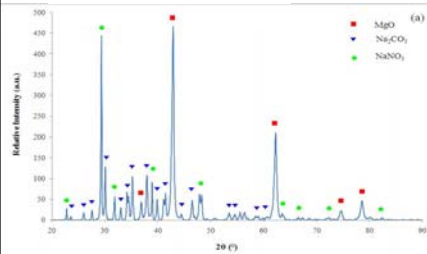
As-prepared absorbent  
(after activation)



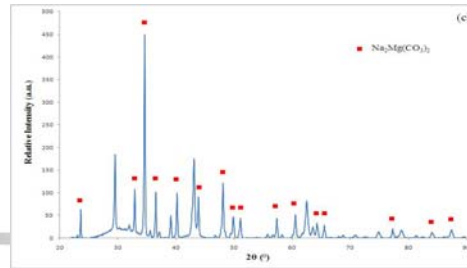
Regenerated absorbent



As-prepared absorbent  
(after activation)

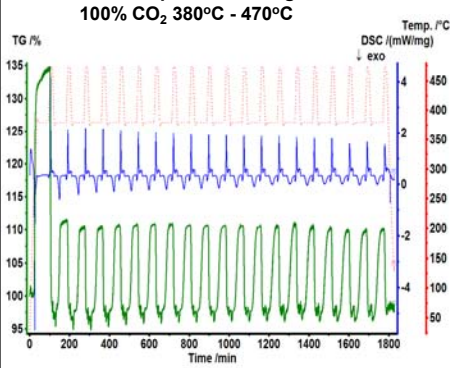


Absorbent loaded with CO<sub>2</sub>

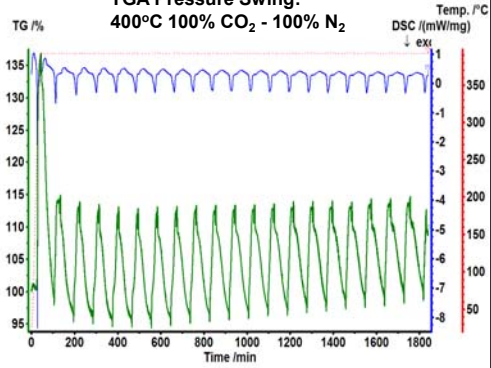


## Performance of MgO-Na<sub>2</sub>CO<sub>3</sub> Warm CO<sub>2</sub> Absorbent

TGA Temperature Swing:  
100% CO<sub>2</sub> 380°C - 470°C



TGA Pressure Swing:  
400°C 100% CO<sub>2</sub> - 100% N<sub>2</sub>



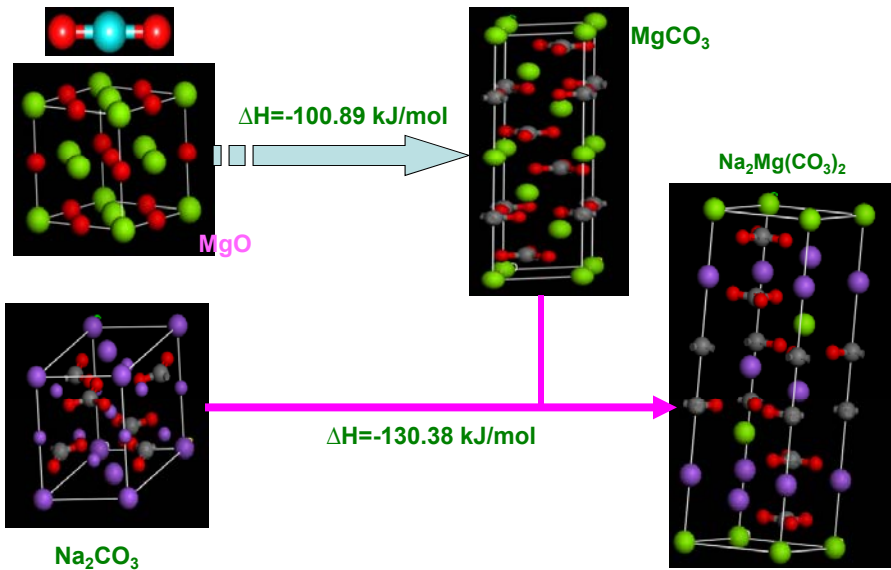
- CO<sub>2</sub> capture capacity: ~15%(wt)
- Easily regenerated both through TSA & PSA.

K. Zhang, et al. submitted to Int. J. Greenhouse Gas Control (2012)

17

NATIONAL ENERGY TECHNOLOGY LABORATORY

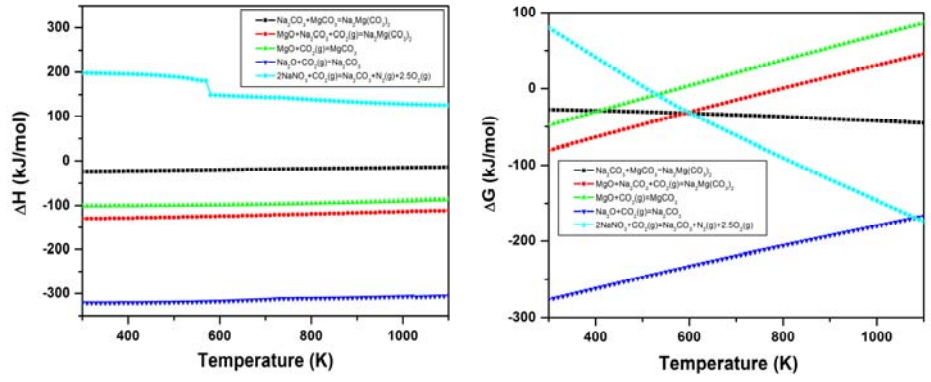
## Na-promoted MgO sorbent



18

NATIONAL ENERGY TECHNOLOGY LABORATORY

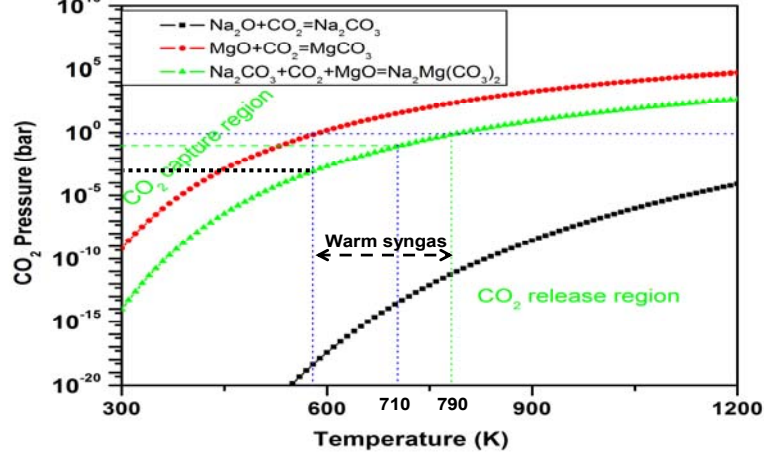
## Na-promoted MgO sorbent



Reaction	$\Delta H$ (kJ/mol) T=300 K	$\Delta G$ (kJ/mol)
$\text{Na}_2\text{O} + \text{CO}_2 = \text{Na}_2\text{CO}_3$	-303.33	-252.86
$\text{MgO} + \text{CO}_2 = \text{MgCO}_3$	-106.05	-52.67
$\text{MgCO}_3 + \text{Na}_2\text{CO}_3 = \text{Na}_2\text{Mg}(\text{CO}_3)_2$	-24.33	-27.90
$\text{MgO} + \text{CO}_2 + \text{Na}_2\text{CO}_3 = \text{Na}_2\text{Mg}(\text{CO}_3)_2$	-130.38	-80.57

NATIONAL ENERGY TECHNOLOGY LABORATORY

## Na-promoted MgO Sorbent



MgO-Na<sub>2</sub>CO<sub>3</sub> mixture: a very promising absorbent for CO<sub>2</sub> removal from warm syngas

NATIONAL ENERGY TECHNOLOGY LABORATORY

## Summary and Conclusions

- Our methodology can be used to search for solid materials with improved CO<sub>2</sub> capture performances. Particularly, it can be used to explore new materials with unknown thermodynamic properties and to Provide guidelines for future experimental design new materials.
- Only promising candidates are needed for experimental tests, which can speed up the searching process and save money;
- Generally, this methodology can be expanded to other classes of solid compounds as well as solutions (*ab initio* +MD).
- The limitations: (a) Need to know the structures of materials with phase transitions; (b) High accurate thermodynamic data (<10 kJ/mol) is not achievable.

21

NATIONAL ENERGY TECHNOLOGY LABORATORY

## Acknowledgement

I would like to express my gratitude for the following colleagues and collaborators for their fruitful discussions, helps and supports in many aspects.

- Dr. D. C. Sorescu (NETL)
- Dr. M. Syamlal (NETL)
- D. Fauth (NETL)
- Dr. R. Siriwardane (NETL)
- Dr. G. Richards (NETL)
- Dr. C. Taylor (NETL)
- Dr. H. P. Loh (NETL)
- R. Anderson (NETL)
- Prof. Karl Johnson (U of Pitt)
- Bo Zhang (U of Pitt)
- Prof. J. W. Halley (UMN)
- Dr. Wei Shi (URS)
- Prof. K. Parlinski (IFJ, Poland)
- Prof. M. J. Janik (PennState U)
- J. Stout (Aeolus Research)

22

NATIONAL ENERGY TECHNOLOGY LABORATORY

## **Thermodynamic Properties of CO<sub>2</sub> Capture Reaction by Solid Sorbents: Theoretical Predictions and Experimental Validations**

Yuhua Duan<sup>1</sup>, David Luebke, Henry Pennline

National Energy Technology Laboratory, United States Department of Energy,  
Pittsburgh, Pennsylvania 15236, USA

Keling Zhang, Xiaohong S. Li, Liyu Li, David King

Institute for Interfacial Catalysis, Pacific Northwest National Laboratory,  
Richland, WA 99354, USA

Lifeng Zhao, Yunhan Xiao

Key Laboratory of Advanced Energy and Power, Institute of Engineering  
Thermodynamics, Chinese Academy of Sciences, Beijing 100190, P. R. China

### **Abstract**

It is generally accepted that current technologies for capturing CO<sub>2</sub> are still too energy intensive. Hence, there is a critical need for development of new materials that can capture CO<sub>2</sub> reversibly with acceptable energy costs. Accordingly, solid sorbents have been proposed to be used for CO<sub>2</sub> capture applications through a reversible chemical transformation. By combining thermodynamic database mining with first principles density functional theory and phonon lattice dynamics calculations, a theoretical screening methodology to identify the most promising CO<sub>2</sub> sorbent candidates from the vast array of possible solid materials has been proposed and validated. The calculated thermodynamic properties of different classes of solid materials versus temperature and pressure changes were further used to evaluate the equilibrium properties for the CO<sub>2</sub> adsorption/desorption cycles. According to the requirements imposed by the pre- and post- combustion technologies and based on our calculated thermodynamic properties for the CO<sub>2</sub> capture reactions by the solids of interest, we were able to screen only those solid materials for which lower capture energy costs are expected at the desired pressure and temperature conditions. These CO<sub>2</sub> sorbent candidates were further considered for experimental validations. In this presentation, we first introduce our screening methodology with validating by solid dataset of alkali and alkaline metal oxides, hydroxides and bicarbonates which thermodynamic properties are available. Then, by studying a series of lithium silicates, we found that by increasing the Li<sub>2</sub>O/SiO<sub>2</sub> ratio in the lithium silicates their corresponding turnover temperatures for CO<sub>2</sub> capture reactions can be increased. Compared to anhydrous K<sub>2</sub>CO<sub>3</sub>, the dehydrated K<sub>2</sub>CO<sub>3</sub>·1.5H<sub>2</sub>O can only be applied for post-combustion CO<sub>2</sub> capture technology at temperatures lower than its phase transition (to anhydrous phase) temperature, which depends on the CO<sub>2</sub> pressure and the steam pressure with the best range being P<sub>H<sub>2</sub>O</sub> ≤ 1.0 bar. Above the phase-transition temperature, the sorbent will be regenerated into anhydrous K<sub>2</sub>CO<sub>3</sub>. Our theoretical investigations on Na-promoted MgO sorbents revealed that the sorption process takes place through formation of the Na<sub>2</sub>Mg(CO<sub>3</sub>)<sub>2</sub> double carbonate with better reaction kinetics over porous MgO, that of pure MgO sorbent. The experimental sorption tests also indicated that the Na-promoted MgO sorbent has high reactivity and capacity towards CO<sub>2</sub> sorption and can be easily regenerated either through pressure or temperature swing processes.

---

<sup>1</sup> Author to whom correspondence should be addressed. Tel. 412-386-5771, Fax 412-386-5920, E-mail: yuhua.duan@netl.doe.gov

## I. Introduction

Carbon dioxide is one of the major combustion products which once released into the air can contribute to the global climate warming effects.<sup>1-3</sup> In order to mitigate the global climate change, CO<sub>2</sub> emissions into the atmosphere must be stopped by separating and capturing CO<sub>2</sub> from coal combustion and gasification plants and sequestering the CO<sub>2</sub> underground. Figure 1 shows a schematic of CO<sub>2</sub> capture, storage and utilization. Among them, CO<sub>2</sub> capture is economically the key step and has three technology routes: (1) post-combustion: capture CO<sub>2</sub> from the flue gas stream after combustion; (2) pre-combustion: capture from the reformed synthesis gas of an upstream gasification unit; (3) oxyfuel: first separation the oxygen from the air and then use of the nearly pure oxygen for fuel combustion to obtain pure CO<sub>2</sub>. Captured CO<sub>2</sub> will be largely sequestered underground. As shown in Figure1, the captured CO<sub>2</sub> also could be used for enhancing oil recovery as well as carbon resources to be converted into other useful compounds<sup>4-6</sup>.

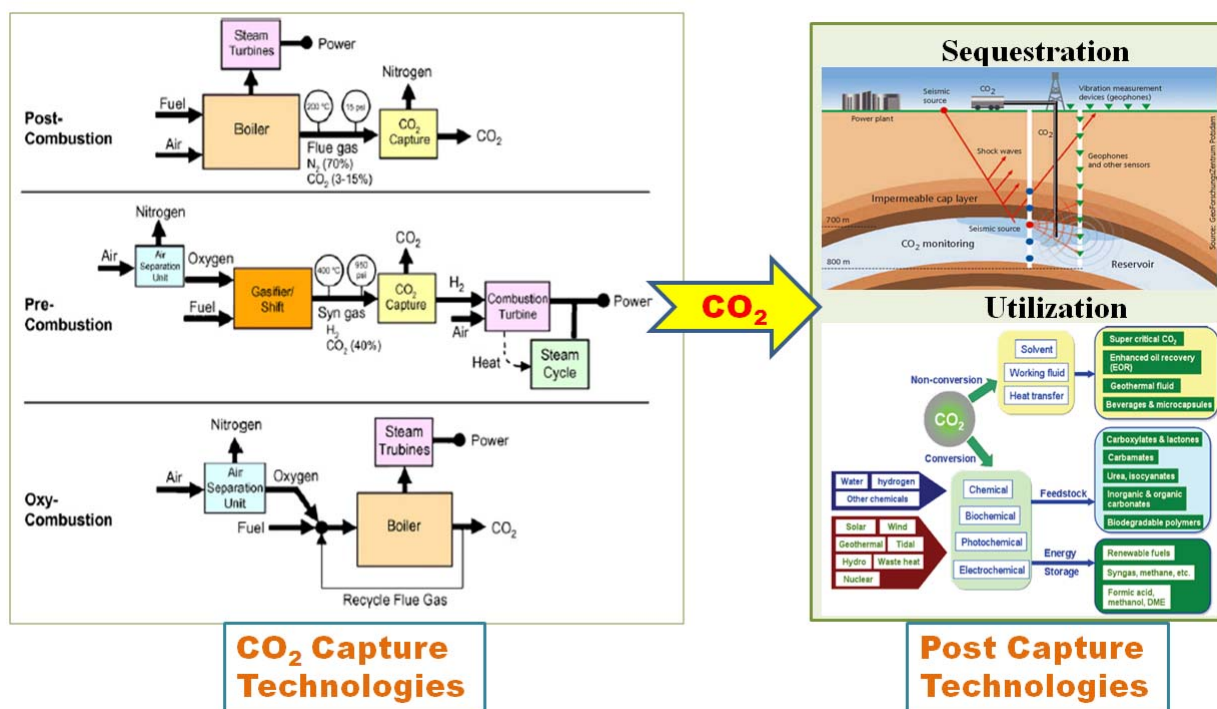


Figure 1. Schematic representation of CO<sub>2</sub> production, capture, storage and utilization<sup>7-9</sup>.

During the past few decades, many efforts have been devoted to new technologies for CO<sub>2</sub> capture, sequestration and utilization.<sup>4-6,10</sup> Current technologies for capturing CO<sub>2</sub> including solvent-based (amines) and CaO-based materials are still too energy intensive. Hence, there is critical need for new materials that can capture and release CO<sub>2</sub> reversibly with acceptable energy costs. Accordingly, solid sorbent materials have been proposed for capturing CO<sub>2</sub> through a reversible chemical transformation and most of them result in the formation of carbonate products. Solid sorbents containing alkali and alkaline earth metals have been reported in several previous studies to be good candidates for CO<sub>2</sub> sorbent applications due to their high CO<sub>2</sub> absorption capacity at moderate working temperatures.<sup>11-13</sup>

To achieve such goals, one of these new methods considered at National Energy Technology Laboratory (NETL) is based on the use of regenerable solid sorbents. In this case sorbents such as alkaline earth metal oxides or hydroxides are used to absorb CO<sub>2</sub> at warm temperatures typically ranging from ~100-300 °C.<sup>14-15</sup> The key phenomenon in these processes is

transformation of the oxide or hydroxide materials to a carbonate upon CO<sub>2</sub> absorption. Regeneration of the sorbent can be obtained, if necessary, in a subsequent step represented by the reverse transformation from the carbonate phase to the oxide or hydroxide phases either through temperature swing or through pressure swing. The efficiencies of these processes are highly dependent on identification of the optimum temperature and pressure conditions at which the absorption and regeneration are performed. In the case of high-performance sorbents, both these two mechanistic steps are optimized in order to achieve minimal energetic and operational costs.

Now the question is how to select promising candidates of good sorbents from vast of solid materials. One way, of course, we can do experimental tests one by one. However, it is very costly and takes long time. Another way is to do the modeling pre-selection to screen out possible best candidates, this list should be shorter. As shown in Fig.2, after computational pre-screening, we only need to do the experimental validation for the short list.

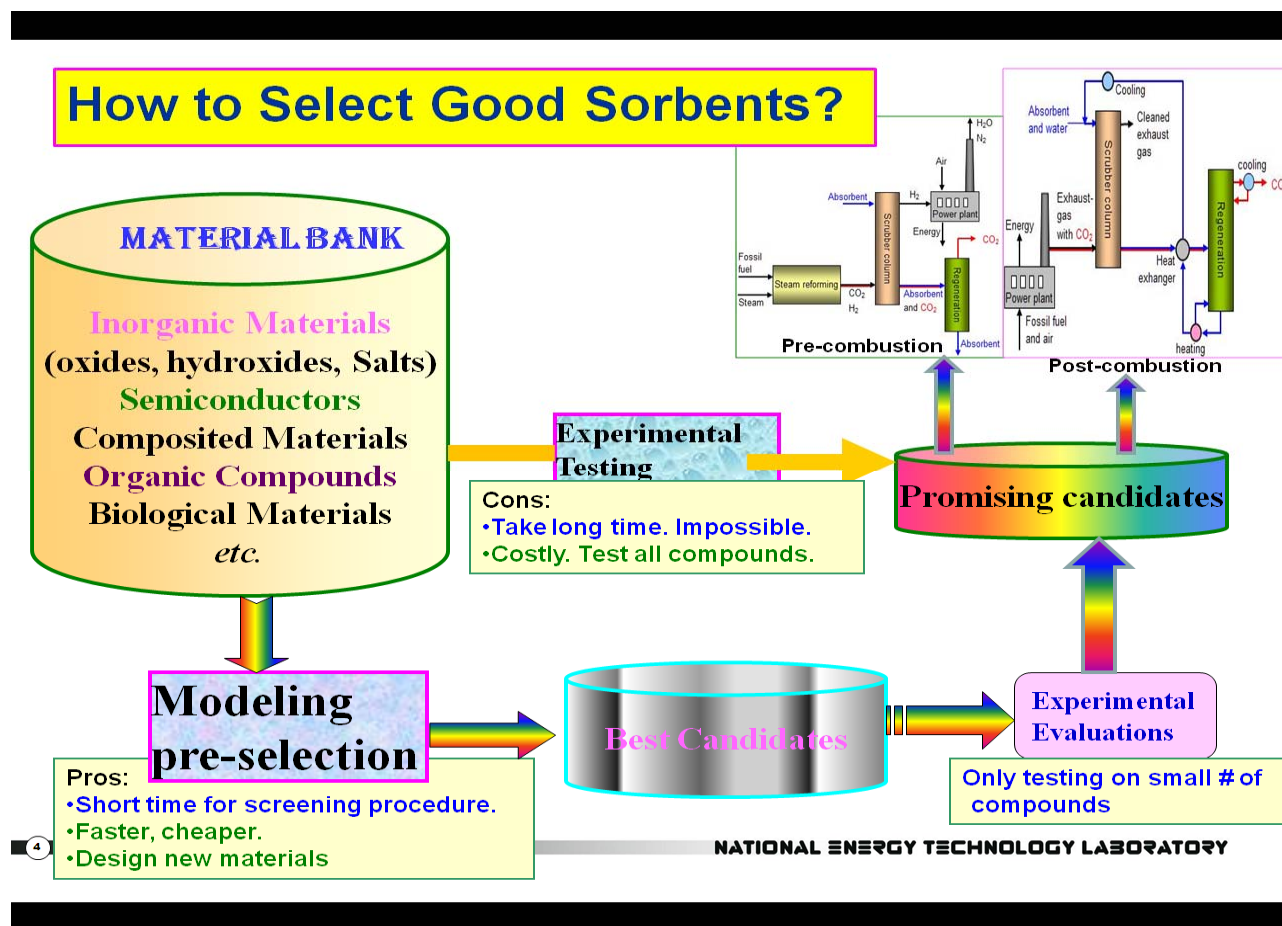


Figure 2. Role of computational modeling in the CO<sub>2</sub> sorbents selection.

Optimization of the sorbent material can be obtained starting from the analysis of its intrinsic atomistic structure and of transformations upon interaction with CO<sub>2</sub>. Of particular importance is to identify the corresponding thermodynamic and kinetic characteristics of the sorbent material of interest. For this purpose scientists at NETL have developed a multi-step computational methodology based on combined use of first principles calculations combined with lattice phonon dynamics to describe the thermodynamic properties of CO<sub>2</sub> capture reactions by solid sorbents.<sup>11,16-22</sup> This methodology has been used to screen different classes of solid

compounds and has, as a major objective, identification of the optimum candidate materials that can be further subjected to experimental testing. The advantage of this proposed method is that it allows identification of the thermodynamic properties of the CO<sub>2</sub> capture reaction as a function of temperature and pressure without any experimental input, except for the crystallographic structural information of the solid phases involved. Such thermodynamic information is essential to guide experimental groups at NETL in development of highly optimized CO<sub>2</sub> sorbents. For a given database of solid materials, our screening scheme allows identification of a short list of promising candidates of CO<sub>2</sub> sorbents with optimal energy usages, which can be further evaluated by our experimental research groups.

In this presentation, we summarize our progress on the development of novel screening scheme to identify most promising candidates for CO<sub>2</sub> sorbents which could be used for either post-combustion or in pre-combustion CO<sub>2</sub> capture technology. The remainder of this report is organized as follows: In the second section we briefly describe the screening method we developed. In the third section, we first provide the validation results of our computational method for the case of alkali and alkaline metal compounds. Then, we present some preliminary results on CO<sub>2</sub> capture reactions by lithium related silicate and zirconate compounds. The main conclusions are summarized in the last section.

## II. Screening Methodology

### 2.1 *ab initio* thermodynamics approach

The complete description of the computational methodology can be found in our previous papers.<sup>11,16-25</sup> Here, we limit ourselves to provide only the main aspects relevant for the current study. The CO<sub>2</sub> capture reactions by solids in the presence of water vapor can be expressed generically in the form



where the terms given in [...] are optional and  $n_1$  and  $n_2$  are the numbers of moles of CO<sub>2</sub> and H<sub>2</sub>O involved in the capture reactions. We treat the gas phase species CO<sub>2</sub> and H<sub>2</sub>O as ideal gases. By assuming that the difference between the chemical potentials ( $\Delta\mu^0$ ) of the solid phases of A, B (and C) can be approximated by the difference in their electronic energies ( $\Delta E^0$ ), obtained directly from first-principles DFT calculations, and the vibrational free energy of the phonons and by ignoring the PV contribution terms for solids, the variation of the chemical potential ( $\Delta\mu$ ) for capture reaction with temperature and pressure can be written as

$$\Delta\mu(T, P) = \Delta\mu^0(T) - RT \ln \frac{P_{\text{CO}_2}^{n_1}}{P_{\text{H}_2\text{O}}^{\pm n_2}} \quad (2)$$

where  $\Delta\mu^0(T)$  is the standard chemical potential changes between reactants and products. If these thermodynamical data are available in the thermodynamic database or literature, we can directly apply them into above equation. If these data are not available, they can be calculated using the *ab initio* thermodynamic approach based on the following approximation.

$$\Delta\mu^0(T) \approx \Delta E^{\text{DFT}} + \Delta E_{\text{ZP}} + \Delta F^{\text{PH}}(T) - n_1 G_{\text{CO}_2}(T) \pm n_2 G_{\text{H}_2\text{O}}(T) \quad (3)$$

Here,  $\Delta E_{\text{ZP}}$  is the zero point energy difference between the reactants and products and can be obtained directly from phonon calculations. The  $\Delta F^{\text{PH}}$  is the phonon free energy change between the solids of products and reactants. If the capture reaction does not involve H<sub>2</sub>O, then the  $P_{\text{H}_2\text{O}}$  in

above equations is set to  $P_0$ , which is the standard state reference pressure of 1 bar, and the  $G_{H_2O}$  term is not present. The “+” and “-” signs correspond to the cases when  $H_2O$  is a product, respectively a reactant, in the general reaction. The free energies of  $CO_2$  ( $G_{CO_2}$ ) and  $H_2O$  ( $G_{H_2O}$ ) can be obtained from standard statistical mechanics. The enthalpy change for the reaction (1),  $\Delta H^{cal}(T)$ , can be derived from above equations as

$$\Delta H^{cal}(T) = \Delta \mu^0(T) + T(\Delta S_{PH}(T) - n_1 S_{CO_2}(T) \pm n_2 S_{H_2O}) \quad (4)$$

In Eq.(3),  $\Delta E^{DFT}$  is the total energy change of the reactants and products calculated by DFT. In this work, the Vienna *Ab-initio* Simulation Package (VASP)<sup>26-27</sup> was employed to calculate the electronic structures of the solid materials involved in this study. All calculations have been done using the projector augmented wave (PAW) pseudo-potentials and the PW91 exchange-correlation functional.<sup>28</sup> This computational level was shown to provide an accurate description of oxide systems.<sup>20-21,29</sup> Plane wave basis sets were used with a cutoff energy of 500 eV and a kinetic energy cutoff for augmentation charges of 605.4 eV. The k-point sampling grids of  $n_1 \times n_2 \times n_3$ , obtained using the Monkhorst-Pack method,<sup>30</sup> were used for these bulk calculations, where  $n_1$ ,  $n_2$ , and  $n_3$  were determined consistent to a spacing of about  $0.028 \text{ \AA}^{-1}$  along the axes of the reciprocal unit cells. In Eqs.(3) and (4), the zero-point-energies( $E_{ZP}$ ), entropies ( $S_{PH}$ ), and harmonic free energies ( $F^{PH}$ , excluding zero-point energy which was already counted into the term  $\Delta E_{ZP}$ ) of solids were calculated by the PHONON software package<sup>31</sup> in which the direct method is applied following the formula derived by Parlinski *et al.*<sup>32</sup> to combine *ab initio* DFT with lattice phonon dynamics calculations.

Based on phonon calculations under the harmonic approximation, the phonon free energy  $\Delta F^{PH}$  change between reactant and product solids can be calculated through the free energy of solids described by the Helmholtz form  $F_{harm}$  as shown in Eq.(2) and the entropy of the solids ( $S_{harm}$ )

$$\Delta F^{PH}(T) = \Delta F_{harm}(T) - T\Delta S_{harm}(T) \quad (5)$$

where the  $F_{harm}$ ,  $S_{harm}$  and the internal energy( $E_{tot}$ ) of the solids are defined as<sup>33</sup>

$$F_{harm}(T) = r k_B T \int_0^\infty g(\omega) \ln[2 \sinh(\frac{\hbar\omega}{2k_B T})] d\omega \quad (6)$$

$$S_{harm}(T) = r k_B \int_0^\infty g(\omega) \{ (\hbar \frac{\hbar\omega}{2k_B T}) [\coth(\frac{\hbar\omega}{2k_B T}) - 1] - \ln[1 - \exp(-\frac{\hbar\omega}{k_B T})] \} d\omega \quad (7)$$

$$E_{tot}(T) = \frac{1}{2} r \int_0^\infty g(\omega) (\hbar\omega) \coth(\frac{\hbar\omega}{2k_B T}) d\omega \quad (8)$$

where  $r$  is the number of degree of freedom in the primitive unit cell. It can be seen that the zero-point-energy ( $E_{ZP}$ ) can be obtained from Eq.(5) by taking  $T \rightarrow 0$ .

$$E_{ZP} = \lim_{T \rightarrow 0} (E_{tot}(T)) \quad (9)$$

where  $\omega$  is the phonon dispersion frequency, and  $g(\omega)$  is the phonon density of state. In this study, we employed the PHONON software package<sup>31</sup> in which the direct method is applied following the formalism derived by Parlinski *et al.*<sup>32</sup> In phonon calculations, a supercell was created from the optimized unit cell structure that was calculated based on DFT. Structures with a displacement of  $0.03 \text{ \AA}$  of non-equivalent atoms were generated from the supercell and DFT calculations were further performed to obtain the force on each atom due to the displacements. These forces were input into the PHONON package<sup>31</sup> to fit the force matrix and further carry out the phonon dispersions and densities, which can be inputted into Eqs.(6)-(8) to calculate the thermodynamic properties.

As an optimal CO<sub>2</sub> solid sorbent, it should not only be easy to absorb CO<sub>2</sub> in the capture cycle but also be easy to release the CO<sub>2</sub> during regeneration cycle. The operating conditions for absorption/desorption processes depend on the sorbent use as in a pre- or a post-combustion application. The US Department of Energy (DOE) programmatic goal for post-combustion and oxy-combustion CO<sub>2</sub> capture is to capture at least 90% of the CO<sub>2</sub> produced by a plant with the cost in electricity increasing no more than 35%, whereas the goal in the case of pre-combustion CO<sub>2</sub> capture is to capture at least 90% of the CO<sub>2</sub> produced with the cost in electricity increasing no more than 10%.<sup>7,34-35</sup> Under pre-combustion conditions, after the water-gas shift reactor, the gas stream mainly contains CO<sub>2</sub>, H<sub>2</sub>O and H<sub>2</sub>. The partial CO<sub>2</sub> pressure could be as high as 20 to 30 bar and the temperature (T<sub>1</sub>) is around 313~573K. To minimize the energy consumption, the ideal sorbents should work in these ranges of pressure and temperature in order to separate CO<sub>2</sub> from H<sub>2</sub>. For post-combustion conditions, the gas stream mainly contains CO<sub>2</sub>, H<sub>2</sub>O, and N<sub>2</sub>, the partial pressure of CO<sub>2</sub> is in the range 0.1 to 0.2 bar, and the temperature (T<sub>2</sub>) range is quite different. Currently, in post-combustion CO<sub>2</sub> capture technology, amine-based solvents, carbon- and zeolite-based solid sorbents (including metal organic framework) capture CO<sub>2</sub> within a lower temperature range (<200°C),<sup>36</sup> while oxides (such as CaO, Na<sub>2</sub>O, *etc.*) and salts (such as Li<sub>4</sub>SiO<sub>4</sub>, Li<sub>2</sub>ZrO<sub>3</sub>, *etc.*) capture CO<sub>2</sub> usually within a higher temperature range (>400°C).<sup>16-20</sup> Based on Eq.(2), the working conditions of each solid capturing CO<sub>2</sub> can be evaluated and used for determining its suitability as CO<sub>2</sub> sorbent.

In this study, the thermodynamic database HSC Chemistry<sup>37</sup> and Factsage<sup>38</sup> packages were employed to search for the available thermodynamic properties of solids.

## 2.2 Screening scheme

Figure 3 shows the schematic of our screening methodology. For a given solid databank, this methodology includes four main screening steps (or filters) which allow identification of the most promising candidates.<sup>20,23</sup>

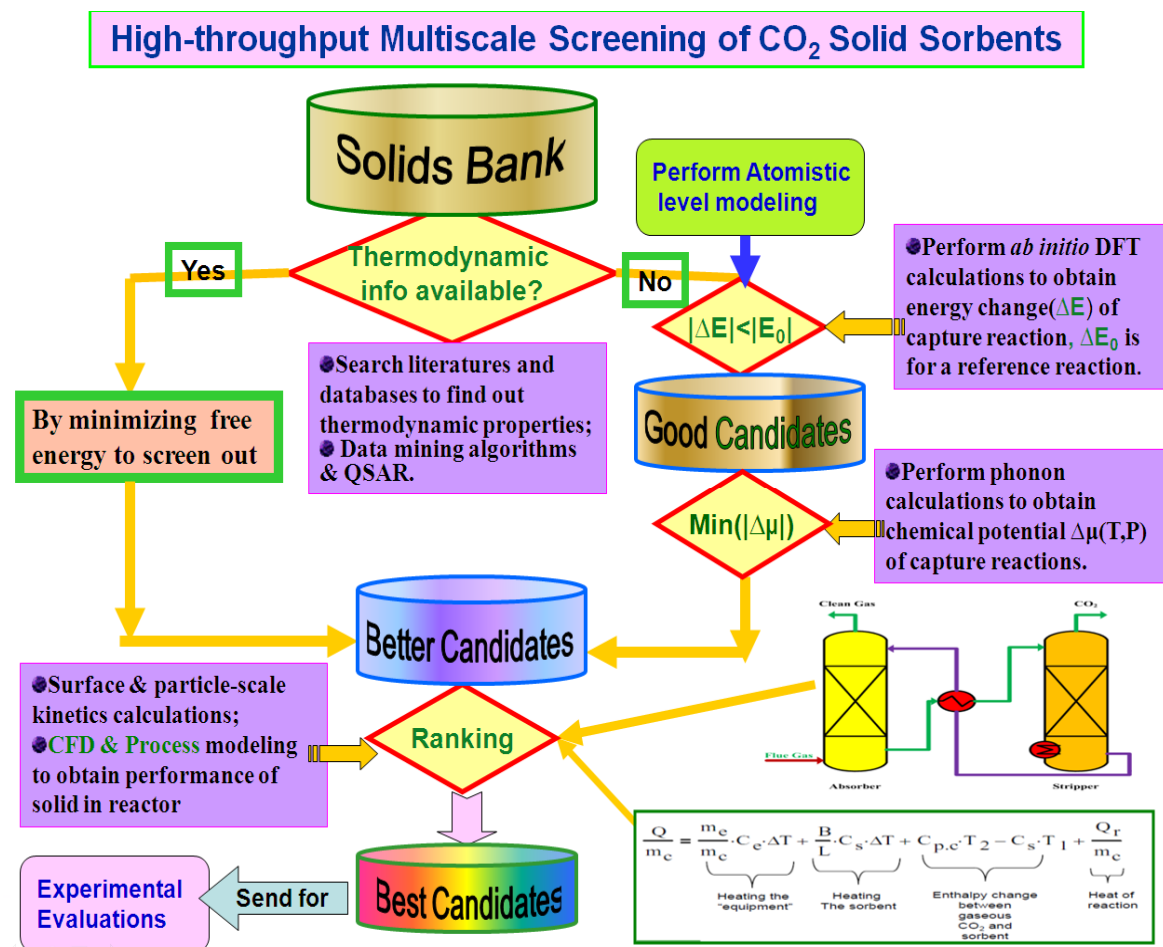
**Step 1:** For each solid in the data bank, we first conduct basic screening based on acquisition of general data, such as the weight percent (wt%) of absorbed CO<sub>2</sub> in the assumption of a complete reaction, the materials safety and cost, *etc.* We also include, where available, the thermodynamic data from literature and from general thermodynamic databases, such as HSC Chemistry, Factsage, *etc.* If the necessary data for evaluation of the thermodynamic properties exists, then the use of DFT calculations is not necessary and the optimal candidates can be obtained by minimizing their known free energies based on the operating conditions. Otherwise, if the material passes basic screening, but no thermodynamic data are available, then we continue to the next step.

**Step 2:** Perform DFT calculations for all compounds in the candidate reaction with this solid. If  $|\Delta E^{\text{DFT}} - \Delta E_{\text{ref}}|/n_1 < 20$  kJ/mol, where  $n_1$  is CO<sub>2</sub> molar number in capture reaction, and  $\Delta E_{\text{ref}}$  is the DFT energy change for the reference capture reaction (*e.g.* CaO+CO<sub>2</sub>=CaCO<sub>3</sub>), we add this compound to the list of good candidates. Otherwise, we go back to *step 1* and pick another solid.

**Step 3:** Perform phonon calculations for reactant and product solids to obtain the corresponding zero point energies and the phonon free energies for the list of good candidates. Specify the target operating conditions (temperature, partial pressures of CO<sub>2</sub> and H<sub>2</sub>O) and compute the change in chemical potential for the reaction, namely  $\Delta\mu(T, P)$  from above equations. If  $\Delta\mu(T, P)$  is close to zero (*e.g.*  $|\Delta\mu(T, P)| < 5$  kJ/mol) at the operating conditions, then we select this reaction as a member of the “better” list. Only a short list of compounds will likely be left after application of *step 3*.

**Step 4:** Additional modeling could be performed to rank the remaining short list of better candidates both obtained from database searching and *ab initio* thermodynamic calculations as shown in figure 1. One is the kinetics of the capture reactions, which could be done by transport and diffusion calculations as well as using experimental measurements. Another necessary and doable

modeling task is the behavior of the solid in the reactor, which can be done by computational fluid dynamics (CFD) methods based on finite element method (FEM) approach and process modeling to estimate the overall costs.<sup>39</sup> These simulations are currently underway. Application of these screening filters will ensure that only the most promising candidates will be identified for the final experimental testing.



This screening methodology provides a path for evaluating materials for which experimental thermodynamic data are unavailable. One area where this approach could be used to great advantage is in evaluating mixtures and doped materials, where thermodynamic data are generally not available but for which the crystallographic structure is known or can be easily determined. Based on the above screening methodology, we have screened hundreds of solid compounds and found some promising candidates for CO<sub>2</sub> sorbents. Here, in this work we summarize the results obtained by applying the screening methodology to several classes of solid materials.

### III. Results and Discussions

#### 3.1 Applications to alkali and alkaline earth metal oxides and hydroxides<sup>11,19-22</sup>

The thermodynamic data for the alkali and alkaline earth metal oxides, hydroxides and corresponding carbonates and bicarbonates are available in thermodynamic databases<sup>37-38</sup>. In order

to validate our theoretical approach, we also made the *ab initio* thermodynamic calculations for these known crystals.

As an example, Figure 4 shows the calculated and experimental measured thermodynamic properties of the reactions for alkali and alkaline earth metal oxides capture of CO<sub>2</sub>. From it, one can see that, except for BeO+CO<sub>2</sub>→BeCO<sub>3</sub> reaction, overall, the calculated results are in good agreement with HSC experimental data. These findings indicate that our theoretical approach can predict the right thermodynamic properties of various solid reacting with CO<sub>2</sub> if the right crystal structure is known or is easy to be determined. The larger discrepancy observed for BeO/BeCO<sub>3</sub> system is due to lack of the crystal structure information of BeCO<sub>3</sub>. As the only one input property of the solid in the *ab initio* thermodynamics calculations, this indicates that in order to obtain reliable results, the crystal structure must be known or can be easily predicted correctly.

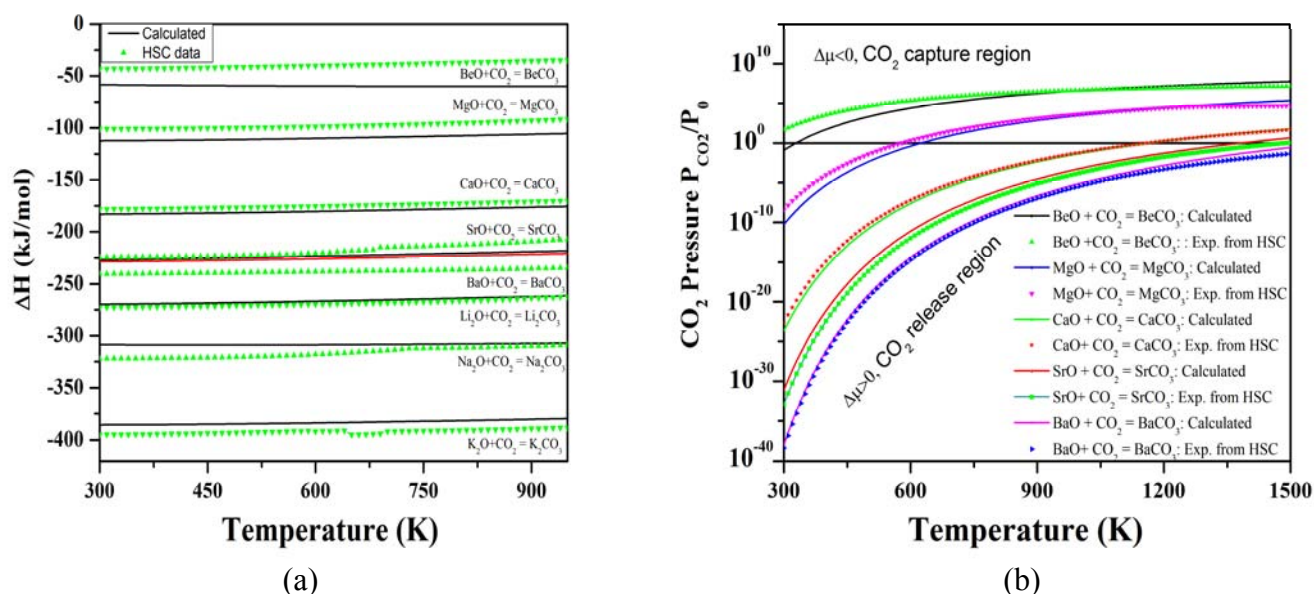


**Figure 4.** (a) The calculated heats of reaction as a function of temperature for eight metal oxides. The solid lines were computed from DFT including phonon contributions. The dashed lines were computed from the HSC package. The discontinuities in the HSC curves indicate phase transitions; (b) The calculated chemical potentials (Gibbs free energy) versus CO<sub>2</sub> pressures (in logarithm scale) and temperatures for the reactions of oxides capturing CO<sub>2</sub> without water involved.

As summarized in Fig.5, among the 24 CO<sub>2</sub> capture reactions of these solids, after applying the first filter (steps 1 & 2), only 10 reactions satisfied our selection criteria and are worth consideration for the third screening step (filter two). After applying the second filter on these 10 reactions, as shown in Fig. 5, we found that only MgO/Mg(OH)<sub>2</sub>, Na<sub>2</sub>CO<sub>3</sub>/NaHCO<sub>3</sub>, K<sub>2</sub>CO<sub>3</sub>/KHCO<sub>3</sub> are promising candidates for CO<sub>2</sub> sorbents in either post-combustion or pre-combustion CO<sub>2</sub> capture technologies.<sup>7,8,10</sup> These results are in good agreement with the experimental facts, which means our screening methodology is reliable and could be used to identify promising solid CO<sub>2</sub> sorbents by predicting the thermodynamic properties of solids reacting with CO<sub>2</sub>.<sup>21</sup>

Based on Eq.(2), Fig. 6 gives the calculated relationships of the chemical potential  $\Delta\mu(T,P)$  with temperature and CO<sub>2</sub> pressure for reactions  $M_2CO_3 + CO_2 + H_2O = 2MHCO_3$  (M=Na, K),  $MgO + CO_2 = MgCO_3$ , and  $Mg(OH)_2 + CO_2 = MgCO_3 + H_2O$ . From Fig. 6, one can see that Na<sub>2</sub>CO<sub>3</sub>/NaHCO<sub>3</sub> and K<sub>2</sub>CO<sub>3</sub>/KHCO<sub>3</sub> can capture CO<sub>2</sub> at low temperature range (400~500K) when CO<sub>2</sub> pressure is around 0.1bar (post-combustion) or 20~30 bar (pre-combustion).<sup>17,21</sup> We have

examined the effect of H<sub>2</sub>O on the reaction thermodynamics and have found that our modeling approach can be used to account for partial pressures of CO<sub>2</sub> and H<sub>2</sub>O and the temperature. We found that formation of bicarbonates from the alkali metal oxides results in a lower sorbent regeneration temperature and that formation of bicarbonate from the carbonates, by addition of CO<sub>2</sub> and H<sub>2</sub>O, reduces the CO<sub>2</sub> capturing temperature even further. Indeed, as shown in Fig.5, we predict that Na<sub>2</sub>CO<sub>3</sub> and K<sub>2</sub>CO<sub>3</sub> have turnover temperatures for CO<sub>2</sub> capture through bicarbonate formation that are suitable for operation under both pre- and post-combustion conditions. When the steam pressure (P<sub>H<sub>2</sub>O</sub>) increases as shown in Fig.6, at the same temperature, the P<sub>CO<sub>2</sub></sub> is decreased because both CO<sub>2</sub> and H<sub>2</sub>O are on the reactant sides.

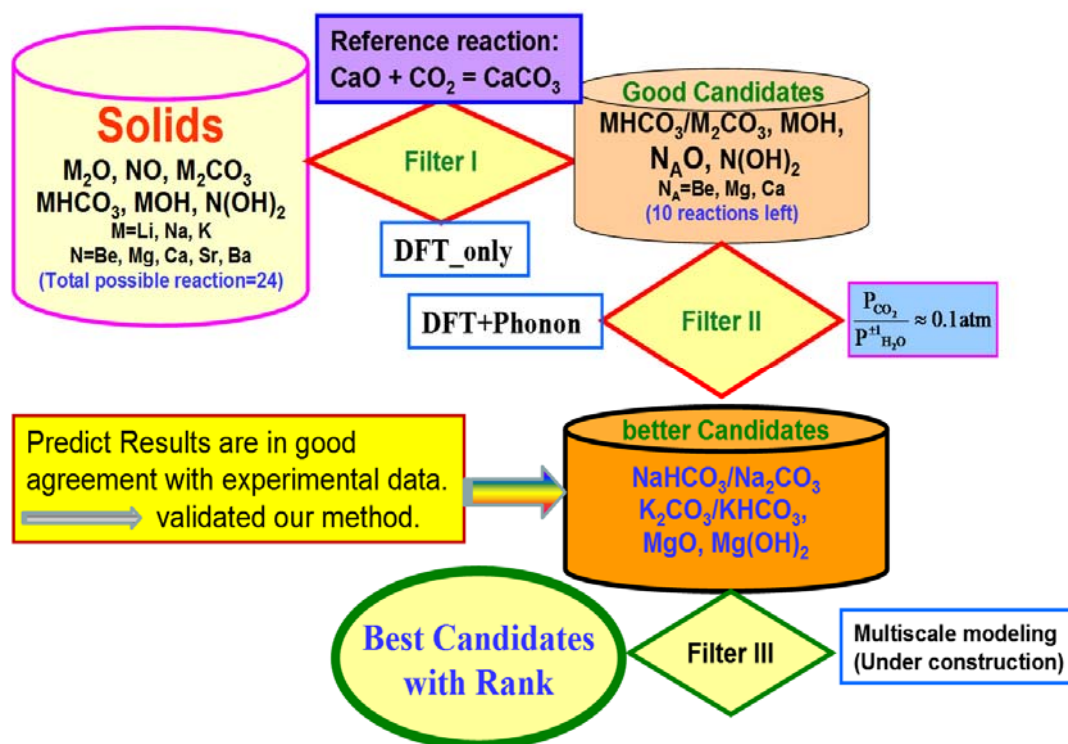


**Figure 5.** Schematic screening results of alkali and alkaline metal oxides, hydroxides and bicarbonates.

As one can see from Fig.6, our results show that MgO could be used for both pre- and post-combustion capture technologies due to its low regenerating temperature ( $T_2=540$  K for post-combustion conditions and  $T_1=690$  K for pre-combustion conditions) which are close to experimental findings. However, Mg(OH)<sub>2</sub> can only be used for post-combustion capture technologies with a turnover  $T_2=600$  K because its turnover temperature ( $T_1$ ) is very high, outside the temperature range of interest for pre-combustion applications.

Among these alkaline-earth metal oxides and hydroxides, comparing with CaO, only MgO and Mg(OH)<sub>2</sub> are found to be good sorbents for CO<sub>2</sub> capture. Upon absorption of CO<sub>2</sub> both of MgO and Mg(OH)<sub>2</sub> can form MgCO<sub>3</sub>. However, the regeneration conditions of the original systems can take place at different conditions as indicated in Fig. 5. In this case we present the calculated phase diagram of MgO-Mg(OH)<sub>2</sub>-MgCO<sub>3</sub> system at different CO<sub>2</sub> pressures and at two fixed P<sub>H<sub>2</sub>O</sub> values (0.1 and 1.0 bar). From Fig.6 it can be seen that when H<sub>2</sub>O is present and at low temperatures, MgCO<sub>3</sub> can release CO<sub>2</sub> to form Mg(OH)<sub>2</sub> instead of forming MgO. For example, at P<sub>H<sub>2</sub>O</sub>=0.1 bar,

only for temperatures under the transition temperature ( $T_{tr}$ ) 460 K,  $MgCO_3$  can be regenerated to form  $Mg(OH)_2$ . By the increase in the  $H_2O$  pressure, the transition temperature is increased. As shown in Fig.5, when  $P_{H_2O}$  is increased to 1.0 bar from 0.1 bar, the corresponding  $T_{tr} = 520K$ . Above  $T_{tr}$ ,  $MgCO_3$  is regenerated to  $MgO$ . Therefore, when water is present in the sorption/desorption cycle, no matter whether the initial sorbent is  $MgO$  or  $Mg(OH)_2$ , and for temperatures below  $T_{tr}$ , the  $CO_2$  capture reaction is dominated by the process  $Mg(OH)_2 + CO_2 \leftrightarrow MgCO_3 + H_2O(g)$ , whereas above  $T_{tr}$ , the  $CO_2$  capture reaction is given by  $MgO + CO_2 \leftrightarrow MgCO_3$ . The reason is that between  $MgO$  and  $Mg(OH)_2$ , there is a phase transition reaction  $MgO + H_2O(g) = Mg(OH)_2$  happening at the transition temperature  $T_{tr}$ . Obviously, by controlling the  $H_2O$  pressure as shown in Fig.6, the  $CO_2$  capture temperature ( $T$  swing) can be adjusted because the  $CO_2$  is a reactant while  $H_2O$  is a product. However, adding more water in the sorbent system will require more energy due to its sensible heat. These results are in good agreement with the experimental measurements.<sup>15</sup>

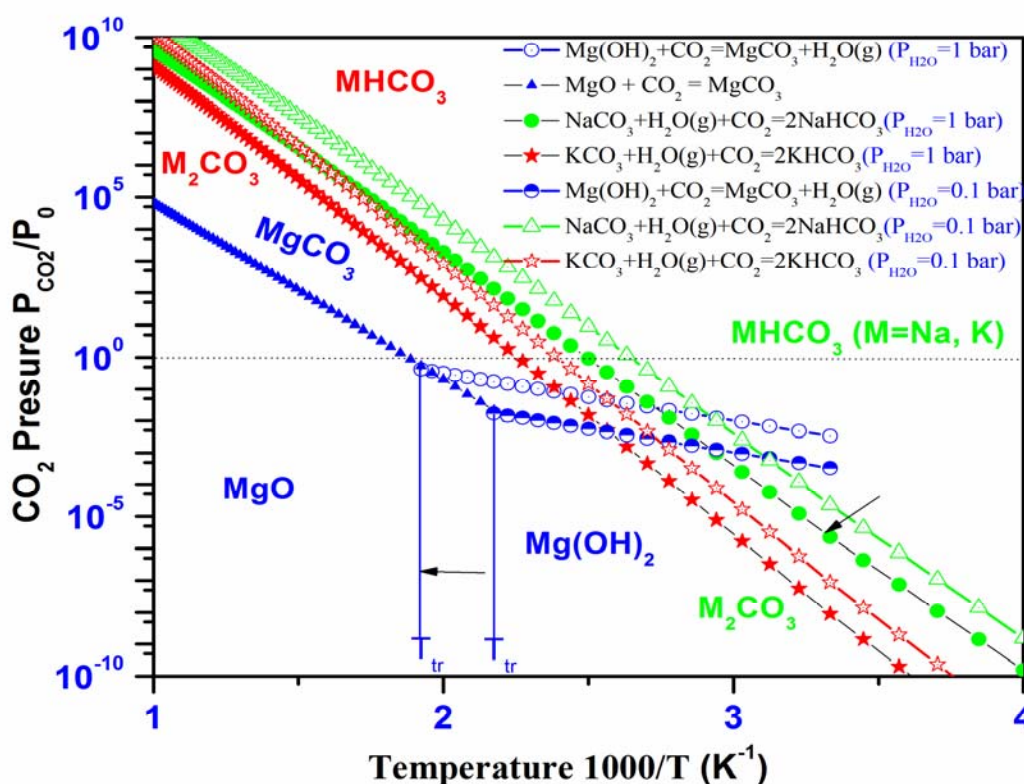


**Figure 6.** The calculated chemical potentials ( $\Delta\mu$ ) versus  $CO_2$  pressure  $P_{CO_2}/P_0$  and temperatures for the reactions of  $MgO$ ,  $Mg(OH)_2$ , and alkali metal carbonates capturing  $CO_2$  at fixed  $P_{H_2O} = 1.0$  bar and 0.1 bar.<sup>20-21</sup> Only the curve with  $\Delta\mu=0$  for each reaction is shown explicitly.

### 3.2 Application to dehydrated and anhydrous potassium carbonates<sup>17,24-25</sup>

Hirano *et al.*<sup>40</sup> and Hayashi *et al.*<sup>41</sup> reported that the formation of active species,  $K_2CO_3 \cdot 1.5H_2O$ , plays an important role in the  $CO_2$  capture capacity and that a vapor pretreatment process substantially improved  $CO_2$  capture capacity.<sup>42</sup> The experimental results showed that the  $CO_2$  capture capacity could be enhanced due to the conversion of the  $K_2CO_3$  phase to the

$\text{K}_2\text{CO}_3 \cdot 1.5\text{H}_2\text{O}$  phase through the  $\text{K}_4\text{H}_2(\text{CO}_3)_3 \cdot 1.5\text{H}_2\text{O}$  phase during pretreatment with sufficient water vapor.<sup>42</sup> Shigemoto and Yanagihara<sup>43</sup> proposed potassium carbonate supported on an activated carbon as an efficient sorbent to recover  $\text{CO}_2$  from moist flue gas through the reaction  $\text{K}_2\text{CO}_3 \cdot 1.5\text{H}_2\text{O} + \text{CO}_2 = 2\text{KHCO}_3 + 0.5\text{H}_2\text{O}$ . However, by using thermogravimetric analysis (TGA) and X-ray diffraction (XRD) measurements to obtain the characteristics of potassium-based sorbents for  $\text{CO}_2$  capture, Zhao *et al.*<sup>44</sup> found that the carbonation reactivity of  $\text{K}_2\text{CO}_3 \cdot 1.5\text{H}_2\text{O}$  and  $\text{K}_2\text{CO}_3$  (in monoclinic structure and dehydrated from  $\text{K}_2\text{CO}_3 \cdot 1.5\text{H}_2\text{O}$ ) was weak, but  $\text{K}_2\text{CO}_3$  (in hexagonal structure) calcined from  $\text{KHCO}_3$  showed excellent carbonation capacity and reproducibility. In order to evaluate the  $\text{CO}_2$  capture performance of  $\text{K}_2\text{CO}_3 \cdot 1.5\text{H}_2\text{O}$  and to compare with the corresponding anhydrous  $\text{K}_2\text{CO}_3$ , we will calculate the thermodynamic properties of  $\text{CO}_2$  capture reactions by  $\text{K}_2\text{CO}_3 \cdot 1.5\text{H}_2\text{O}$  and  $\text{K}_2\text{CO}_3$  to find the optimal working conditions for achieving maximum capture capacity.

According to Eq.(3), the calculated heats of reaction (enthalpy change) for these two reactions versus temperature are plotted in Fig.7(a). Obviously, along the temperature range, the anhydrous  $\text{K}_2\text{CO}_3$  capture of  $\text{CO}_2$  can release more reaction heat than the hydrated  $\text{K}_2\text{CO}_3 \cdot 1.5\text{H}_2\text{O}$ . This means the interaction of  $\text{K}_2\text{CO}_3$  with  $\text{CO}_2$  is much stronger than that of  $\text{K}_2\text{CO}_3 \cdot 1.5\text{H}_2\text{O}$ , and during the regeneration stage, more energy is required to regenerate  $\text{K}_2\text{CO}_3$ . With  $P_{\text{gas}}=1$  bar, Fig.7(b) shows the calculated Gibbs free energy of these two reactions versus temperature. The slope of the free energy versus temperature for reaction  $\text{K}_2\text{CO}_3 + \text{H}_2\text{O}(\text{g}) + \text{CO}_2 = 2\text{KHCO}_3$  is larger than that of  $\text{K}_2\text{CO}_3 \cdot 1.5\text{H}_2\text{O} + \text{CO}_2 = 2\text{KHCO}_3 + 0.5\text{H}_2\text{O}(\text{g})$ . This indicates that the driving force for  $\text{K}_2\text{CO}_3$  to capture a  $\text{CO}_2$  is larger than that of  $\text{K}_2\text{CO}_3 \cdot 1.5\text{H}_2\text{O}$ , and the energy ( $\Delta G > 0$ ) needed to reverse the reaction  $\text{K}_2\text{CO}_3 + \text{H}_2\text{O}(\text{g}) + \text{CO}_2 = 2\text{KHCO}_3$  is larger than that the reaction  $\text{K}_2\text{CO}_3 \cdot 1.5\text{H}_2\text{O} + \text{CO}_2 = 2\text{KHCO}_3 + 0.5\text{H}_2\text{O}(\text{g})$ .

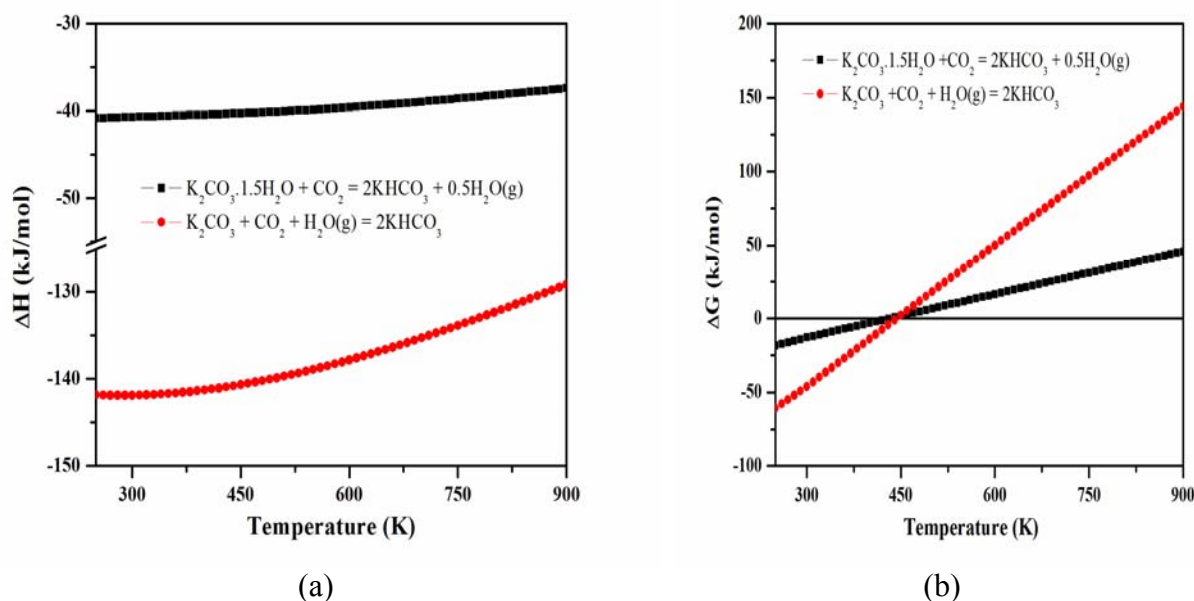


**Figure 7.** The calculated thermodynamic properties of  $\text{K}_2\text{CO}_3 \cdot 1.5\text{H}_2\text{O}$  and  $\text{K}_2\text{CO}_3$  reacting with  $\text{CO}_2$ . (a) Heat of reaction versus temperature; (b) Gibbs free energy versus temperature.<sup>24</sup>

By examining Eq.(2), for the reactions of  $\text{K}_2\text{CO}_3 \cdot 1.5\text{H}_2\text{O}$  capturing  $\text{CO}_2$ , we can explore the relationship among chemical potential ( $\Delta\mu(T,P)$ ), temperature, and  $\text{CO}_2$  pressure ( $P_{\text{CO}_2}$ ) at several fixed  $P_{\text{H}_2\text{O}}$ . This kind of relationship for these two reactions is shown in Fig.8 as a contour plot in a two dimensional representation. The lines in Fig.8 indicate conditions at which the  $\Delta\mu(T,P)$  is zero.

Near to these lines is a good region for energy efficient absorption and desorption because of the minimal energy costs at the given temperature and pressure. Above these lines in Fig.8 ( $\Delta\mu(T,P)<0$ ), the solids  $K_2CO_3 \cdot 1.5H_2O$  and  $K_2CO_3$  are respectively favored to absorb  $CO_2$  and to form  $KHCO_3$ , while below these lines ( $\Delta\mu(T,P)>0$ ) the  $KHCO_3$  is favored to release  $CO_2$  regenerating the solid sorbent.

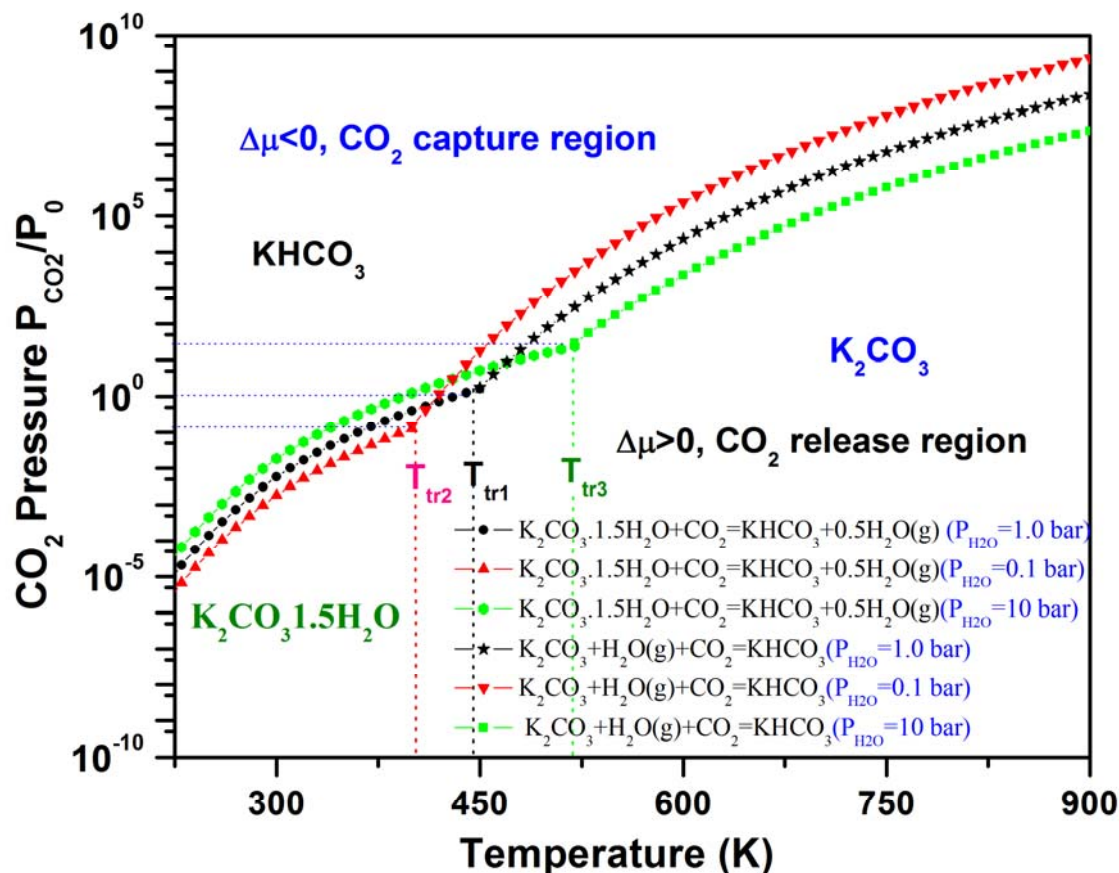


**Figure 8.** The contour plots of the calculated chemical potentials ( $\Delta\mu$ ) versus temperatures and  $CO_2$  pressures at several fixed  $H_2O$  pressures and temperatures for  $K_2CO_3 \cdot 1.5H_2O$  and  $K_2CO_3$  capturing  $CO_2$ . Y-axis is given in logarithmic scale. Only  $\Delta\mu=0$  curves with different fixed  $P_{H_2O}$  are shown explicitly. For each reaction, above the  $\Delta\mu=0$  curve, the carbonates absorb  $CO_2$  and the reaction goes forward ( $\Delta\mu < 0$  region) to form bicarbonate, whereas below the  $\Delta\mu=0$  curve, the bicarbonate release  $CO_2$  and the reaction goes backward to regenerate the carbonates ( $\Delta\mu > 0$  region).

From Fig.8 one can see that at each fixed  $P_{H_2O}$  these two lines of the reactions for  $K_2CO_3 \cdot 1.5H_2O$  and  $K_2CO_3$  capturing  $CO_2$  cross at a transition temperature ( $T_{tr}$ ), which means that at this temperature there is a phase transition  $K_2CO_3 \cdot 1.5H_2O \leftrightarrow K_2CO_3 + 1.5H_2O$  happening. Obviously, at each fixed  $P_{H_2O}$ , the  $T_{tr}$  is fixed and does not depend on  $P_{CO_2}$  as shown with vertical line in Fig.8. Therefore, in Fig.8 the phase-diagram has three regions corresponding to three solid phases: the region below  $T_{tr}$  and under the line is  $K_2CO_3 \cdot 1.5H_2O$ , the region above  $T_{tr}$  and under the line is

$K_2CO_3$ , while the rest region above the lines is the  $KHCO_3$  phase. In other words, below  $T_{tr}$  only  $K_2CO_3 \cdot 1.5H_2O$  could be regenerated, while above  $T_{tr}$  the anhydrous  $K_2CO_3$  could be regenerated. Table 1 summarizes the obtained results.

**Table 1.** The calculated thermodynamic properties of reactions of  $CO_2$  captured by hydrated and dehydrated potassium carbonates in the unit of  $kJ/mol$ .<sup>24</sup> The highest temperature for carbonates capturing  $CO_2$  at pre-combustion ( $T_1$ ) ( $P_{CO_2}=20$  bar) and post-combustion ( $T_2$ ) ( $P_{CO_2}=0.1$  bar) conditions as well as the phase transition temperature ( $T_{tr}$ ) of  $K_2CO_3 \cdot 1.5H_2O$  into  $K_2CO_3$  are also given in this Table.

Reactions	$CO_2$ wt%	$\Delta E_{DFT}$	$\Delta E_{ZP}$	$\Delta H$ (T=300K)	$\Delta G$ (T=300K)	$T_1$ (K)	$T_2$ (K)	$T_{tr}$ (K)
$K_2CO_3 \cdot 1.5H_2O + CO_2 = 2KHCO_3 + 0.5H_2O(g)$	26.88	-40.474	-0.737	-40.678	-12.820	580 <sup>b</sup> 665 <sup>c</sup> 510 <sup>d</sup>	370 <sup>b</sup> 395 <sup>c</sup> 335 <sup>d</sup>	445 <sup>b</sup> 395 <sup>c</sup> 515 <sup>d</sup>
$K_2CO_3 + CO_2 + H_2O(g) = 2KHCO_3$	31.84	-154.429	18.293	-141.728 -142.854 <sup>a</sup>	-46.281 -44.716 <sup>a</sup>	490 <sup>b</sup> 455 <sup>c</sup> 515 <sup>d</sup>	420 <sup>b</sup> 395 <sup>c</sup> 445 <sup>d</sup>	

<sup>a</sup> Calculated by HSC Chemistry package<sup>37</sup>

<sup>b</sup> when  $P_{H_2O} = 1$  bar

<sup>c</sup> when  $P_{H_2O} = 0.1$  bar

<sup>d</sup> when  $P_{H_2O} = 10$  bar

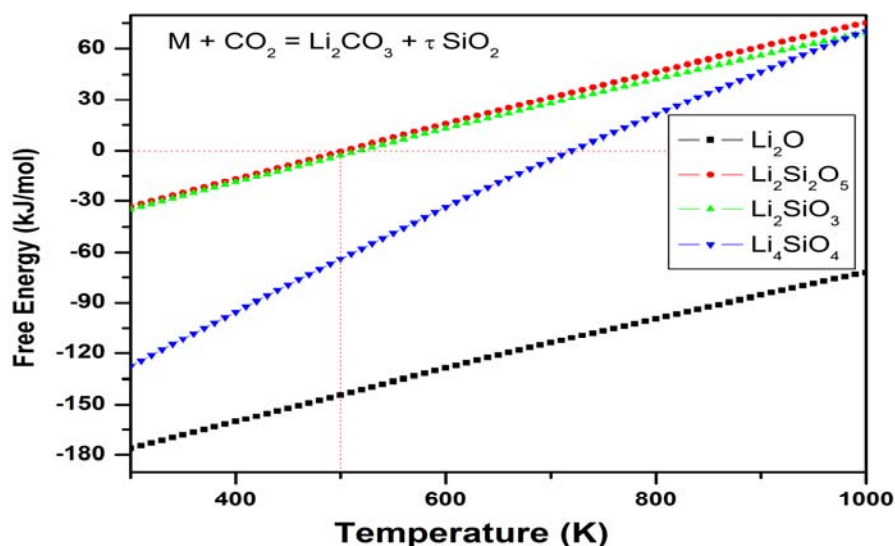


**Figure 9.** The Gibbs free energy changes of some lithium silicates capture  $CO_2$  reactions from HSC Chemistry database.<sup>37</sup>

### 3.3 Applications to mixture of solids<sup>16-18,22</sup>

Lithium silicate ( $Li_4SiO_4$ ) and zirconate ( $Li_2ZrO_3$ ) have been proposed experimentally as promising high-temperature  $CO_2$  sorbents.<sup>45-51</sup> And our previous theoretical studies confirmed these findings.<sup>16-18</sup> Figure 8 shows the free energy changes of  $CO_2$  capture reactions by some lithium silicates as obtained from HSC Chemistry database. From Fig. 9, one can see that comparing with  $Li_2O$ ,  $Li_4SiO_4$ , and  $Li_2ZrO_3$ , the  $Li_2SiO_3$ ,  $Li_2Si_2O_5$ , and  $Li_2Si_2O_7$  are better  $CO_2$  solid sorbent

candidates because they require less free energy to reverse the CO<sub>2</sub> capture reactions and have lower regenerating temperatures. Our calculations show that although pure Li<sub>2</sub>O can absorb CO<sub>2</sub> efficiently, it is not a good solid sorbent for CO<sub>2</sub> capture because the reverse reaction, corresponding to Li<sub>2</sub>CO<sub>3</sub> releasing CO<sub>2</sub>, can only occur at very low CO<sub>2</sub> pressure and/or at very high temperature.<sup>19</sup> SiO<sub>2</sub> does not interact with CO<sub>2</sub> at normal conditions. Therefore, it can be concluded that when a lithium silicate compound with the ratio of Li<sub>2</sub>O/SiO<sub>2</sub> is less or equal to 1.0, it could have better CO<sub>2</sub> capture performance than Li<sub>4</sub>SiO<sub>4</sub>, because its regeneration can occur at low temperature and hence require less regeneration heat. Further calculations (steps 3 and 4) and analysis on these lithium silicates capture CO<sub>2</sub> properties are underway.

Figure 10(a) summarizes our calculated heats of reaction ( $\Delta H$ ) for an alkali metal silicate and three zirconates.<sup>16-18</sup> From Fig. 10(a), one can see that the K<sub>2</sub>ZrO<sub>3</sub> capture of CO<sub>2</sub> has a larger  $\Delta H$  than the other three solids. Li<sub>4</sub>SiO<sub>4</sub> has a relative small  $\Delta H$  while along a large temperature range the Li<sub>2</sub>ZrO<sub>3</sub> and Na<sub>2</sub>ZrO<sub>3</sub> have similar  $\Delta H$ . Therefore, K<sub>2</sub>ZrO<sub>3</sub> is not a good CO<sub>2</sub> sorbent candidate because it needs more heat to regenerate. Among these four solids, Li<sub>4</sub>SiO<sub>4</sub> is the best choice. These results are in good agreement with available experimental measurements.<sup>45-51</sup>

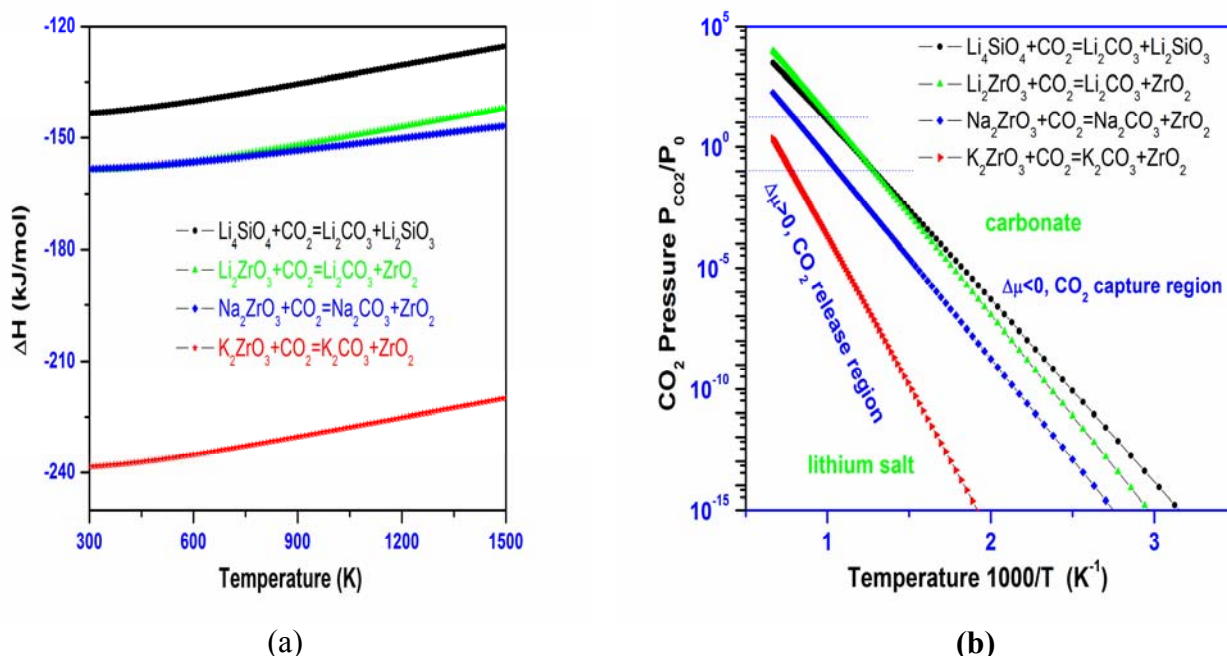


**Figure 10.** The calculated thermodynamic properties of some alkali metal silicate and zirconates capture CO<sub>2</sub>.<sup>16-18</sup> (a) The heat of reactions; (b) the contour plotting of calculated chemical potentials ( $\Delta\mu$ ) versus CO<sub>2</sub> pressures and temperatures of the sorbents capture CO<sub>2</sub> reactions. Y-axis plotted in logarithm scale. Only  $\Delta\mu=0$  curve is shown explicitly. For each reaction, above its  $\Delta\mu=0$  curve, their  $\Delta\mu < 0$ , which means the sorbents absorb CO<sub>2</sub> and the reaction goes forward, whereas below the  $\Delta\mu=0$  curve, their  $\Delta\mu > 0$ , which means the CO<sub>2</sub> start to release and the reaction goes backward to regenerate the sorbents.

According to Eq.(2), the calculated relationships of  $\Delta\mu$  with CO<sub>2</sub> pressure and temperature for these four solids are shown in Fig.10(b). The line in Fig.10(b) indicates that for each reaction,  $\Delta\mu(T, P)$  is approaching zero. The region close to the line is favorable for the absorption and desorption because of the minimal energy costs at a given temperature and pressure. Above the line, the solid (Li<sub>4</sub>SiO<sub>4</sub>, M<sub>2</sub>ZrO<sub>3</sub> (M=Li, Na, K)) is favorable to absorb CO<sub>2</sub> and to form Li<sub>2</sub>CO<sub>3</sub>, while

below the line the  $\text{Li}_2\text{CO}_3$  is favorable to release  $\text{CO}_2$  and to regenerate to lithium silicate solids. The calculated thermodynamic properties of these solids are also summarized in Table 2.

From Fig.10(b) and Table 2 one can see that these solids capture  $\text{CO}_2$  up to higher temperatures ( $T_1 > 1000\text{K}$ ) compared with the desired pre-combustion condition (313~573K). Therefore, they are not good sorbents for capturing  $\text{CO}_2$  in pre-combustion technology. However, some of them could be used for high-temperature post-combustion  $\text{CO}_2$  capture technology with  $T_2 = 1285\text{K}$ , 925 K, 780K, and 770K for  $\text{K}_2\text{ZrO}_3$ ,  $\text{Na}_2\text{ZrO}_3$ ,  $\text{Li}_2\text{ZrO}_3$  and  $\text{Li}_4\text{SiO}_4$  respectively. Obviously, compared to  $\text{CaO}$ , the  $T_2$  of  $\text{K}_2\text{ZrO}_3$  is still too high to be used for post-combustion technology. This may be part of the reason that there is no experimental work found in the literature for pure  $\text{K}_2\text{ZrO}_3$  capturing  $\text{CO}_2$ . Therefore,  $\text{Li}_4\text{SiO}_4$ ,  $\text{Na}_2\text{ZrO}_3$ , and  $\text{Li}_2\text{ZrO}_3$  are good candidates for  $\text{CO}_2$  sorbents working at high temperature.

**Table 2.** The summary of the calculated energy change  $\Delta E^{\text{DFT}}$ , the zero-point energy changes  $\Delta E_{\text{ZP}}$  and the thermodynamic properties ( $\Delta H$ ,  $\Delta G$ ) of the  $\text{CO}_2$  capture reactions by alkali metal silicates and zirconates. (unit: kJ/mol).<sup>16-18,20</sup> The turnover temperatures ( $T_1$  and  $T_2$ ) of the reactions of  $\text{CO}_2$  capture by solids under the conditions of pre-combustion ( $P_{\text{CO}_2} = 20$  bar) and post-combustion ( $P_{\text{CO}_2} = 0.1$  bar) are also listed.

Reaction	$\Delta E^{\text{DFT}}$	$\Delta E_{\text{ZP}}$	$\Delta H$ (T=300K)	$\Delta G$ (T=300K)	Turnover T (K)	
					$T_1$	$T_2$
$\text{Li}_4\text{SiO}_4 + \text{CO}_2 \leftrightarrow \text{Li}_2\text{CO}_3 + \text{Li}_2\text{SiO}_3$	-148.704	5.971	-143.548	-93.972	1010	770
$\text{Li}_2\text{ZrO}_3 + \text{CO}_2 \leftrightarrow \text{Li}_2\text{CO}_3 + \text{ZrO}_2$	-146.648	11.311	-158.562 -162.69 <sup>a</sup>	-103.845 -113.18 <sup>a</sup>	1000	780
$\text{K}_2\text{ZrO}_3 + \text{CO}_2 \leftrightarrow \text{K}_2\text{CO}_3 + \text{ZrO}_2$	-223.158	5.813	-238.490	-187.884	hT <sup>b</sup>	1285
$\text{Na}_2\text{ZrO}_3 + \text{CO}_2 \leftrightarrow \text{Na}_2\text{CO}_3 + \text{ZrO}_2$	-140.862	2.236	-158.327 -151.403 <sup>a</sup>	-114.121 -105.252 <sup>a</sup>	1275	925

<sup>a</sup> from HSC-Chemistry database package<sup>16</sup>

<sup>b</sup> hT means the temperature is higher than our temperature range (1500 K)

Although  $\text{Li}_4\text{SiO}_4$  and  $\text{Li}_2\text{ZrO}_3$  have similar turnover temperature  $T_2$  as shown in Table 2, from Fig.10(a) one can see that the reaction heat of  $\text{Li}_2\text{ZrO}_3$  capture of  $\text{CO}_2$  is about 20 kJ/mol lower than that of  $\text{Li}_4\text{SiO}_4$ . This indicates that more heat is needed for regenerating  $\text{Li}_2\text{ZrO}_3$  from  $\text{Li}_2\text{CO}_3$  and  $\text{ZrO}_2$ . Therefore, as a  $\text{CO}_2$  sorbent, the  $\text{Li}_4\text{SiO}_4$  is thermodynamically better than  $\text{Li}_2\text{ZrO}_3$ , despite they may have different kinetics behaviors.<sup>52</sup>

### 3.4 Application to double salt materials<sup>53</sup>

In pre-combustion capture with combined warm syngas cleanup, the operating temperature is 300-400 °C.  $\text{MgO}$  based double salt based material has a unique working temperature falling in this temperature range and fits in many processes such as IGCC and sorption-enhanced reaction for hydrogen production.<sup>53-54</sup> Thermodynamically, pure  $\text{MgO}$  can react and combine with  $\text{CO}_2$  up to 300 °C to form  $\text{MgCO}_3$ , which falls at the lower end of the desired temperature range (300-400 °C).

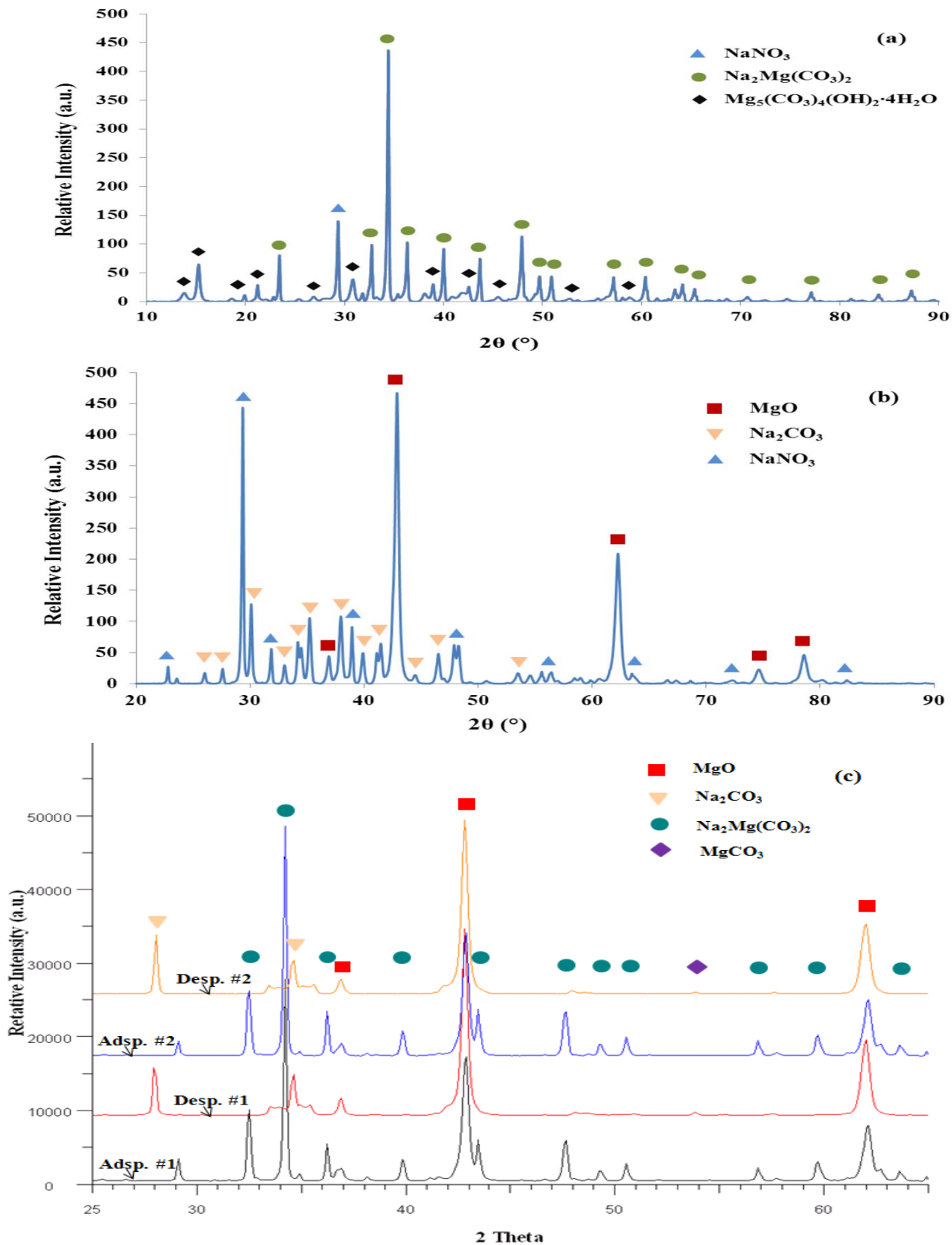


**Figure 11.** X-ray diffraction patterns of Na<sub>2</sub>CO<sub>3</sub>-promoted MgO sorbent: (a) pre-activated; (b) post-activated; (c) during absorption cycles.

In addition, MgO shows a very low capacity of 0.24 mmol/g CO<sub>2</sub> capture at 200 °C and remains difficult to regenerate.<sup>55-56</sup> Lower capacity and difficulty to regenerate limit its practical application as a CO<sub>2</sub> absorbent for warm gas cleans up. An MgO based double salt was reported to have a high capacity of 11mmol/g at the temperature of 375 °C and became a very promising intermediate temperature CO<sub>2</sub> absorbent.<sup>54</sup> As shown in Fig.11, the MgO promoted by Na<sub>2</sub>CO<sub>3</sub> showed a double salt Na<sub>2</sub>Mg(CO<sub>3</sub>)<sub>2</sub> was formed after capturing CO<sub>2</sub> and could be regenerated at higher temperature compared to the case of pure MgO.<sup>53</sup> More detailed experimental measured results will be presented at this conference as well as be included in this conference's proceedings.<sup>57</sup>

Since the thermodynamic properties of double salt Na<sub>2</sub>Mg(CO<sub>3</sub>)<sub>2</sub> are not available, by applying our modeling technology as described in section 2, we calculated its electronic and thermodynamic properties versus temperature. In table 3 list the heat of reaction ( $\Delta H$ ) of MgO and MgO+Na<sub>2</sub>CO<sub>3</sub> capture CO<sub>2</sub>. Compared with pure MgO capturing CO<sub>2</sub> to form MgCO<sub>3</sub>, as one can see by forming double salt, the  $\Delta H$  is about 28 kJ/mol lower, which corresponds to higher regenerating temperature. Fig.12 shows the thermodynamic properties of the reactions studied in this paper calculated from HSC Chemistry database and *ab initio* thermodynamic approach. From it one can see that with increasing temperature the  $\Delta H(T)$  and  $\Delta G(T)$  of MgO+Na<sub>2</sub>CO<sub>3</sub> capture CO<sub>2</sub> reaction are always lower than those of pure MgO capturing CO<sub>2</sub>, but higher than those of pure Na<sub>2</sub>O capturing CO<sub>2</sub>.

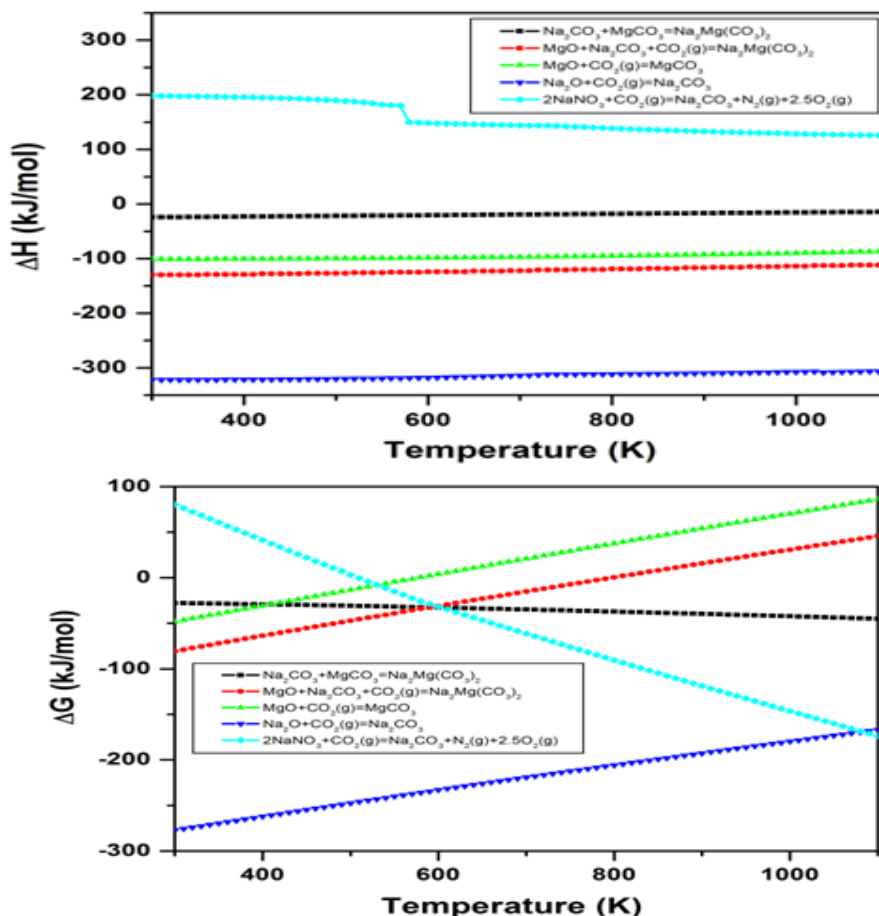


**Figure 12.** The thermodynamic properties of the reactions studied in this paper calculated from HSC Chemistry database and *ab initio* thermodynamic approach: (a) Enthalpy change versus temperatures; (b) Gibbs free energy change versus temperatures.

**Table 3.** The calculated heat of reaction for MgO and MgO+Na<sub>2</sub>CO<sub>3</sub> capture CO<sub>2</sub>

Reaction	$\Delta H$ (kJ/mol)
$\text{MgO} + \text{CO}_2 = \text{MgCO}_3$	-92.51
$\text{MgCO}_3 + \text{Na}_2\text{CO}_3 = \text{Na}_2\text{Mg}(\text{CO}_3)_2$	-27.68
$\text{MgO} + \text{CO}_2 + \text{Na}_2\text{CO}_3 = \text{Na}_2\text{Mg}(\text{CO}_3)_2$	-120.19

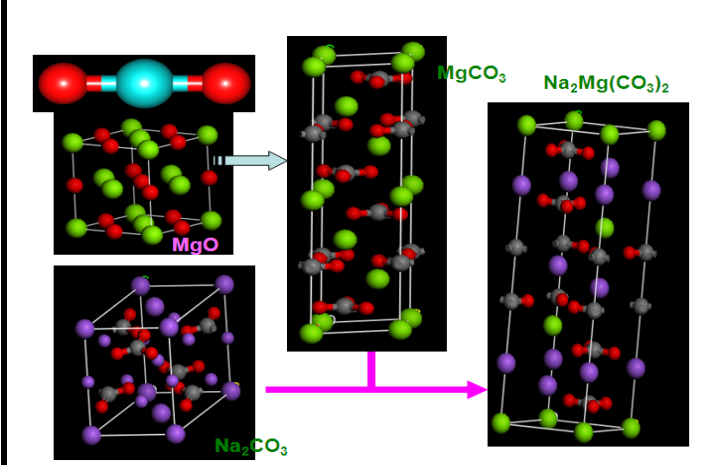
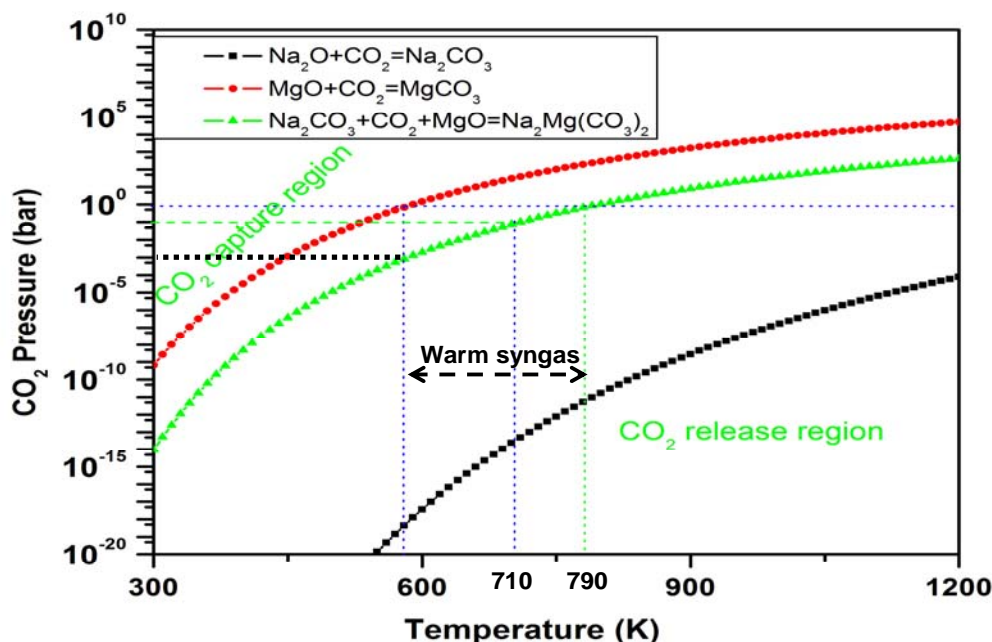


Fig. 13 shows the calculated chemical potential ( $\Delta\mu$ ) versus temperature and the CO<sub>2</sub> pressure for the CO<sub>2</sub> capture reactions by Na<sub>2</sub>O, MgO, and Na<sub>2</sub>CO<sub>3</sub>+MgO. Clearly, the MgO+Na<sub>2</sub>CO<sub>3</sub> sorbent falls in the temperature range of the warm syngas cleanup. Therefore, it is a good candidate for CO<sub>2</sub> capture at warm temperature.



**Figure 13.** The contour plotting of calculated chemical potential ( $\Delta\mu$ ) versus temperature and the CO<sub>2</sub> pressure for the CO<sub>2</sub> capture reactions by Na<sub>2</sub>O, MgO, and Na<sub>2</sub>CO<sub>3</sub>+MgO.

## 4 Conclusions

By combining thermodynamic database searching with first principles density functional theory and phonon lattice dynamics calculations, with a vast array of solid materials, we proposed a theoretical screening methodology to identify promising candidates for CO<sub>2</sub> sorbents. The

thermodynamic properties of solid materials are obtained and used for computing the thermodynamic reaction equilibrium properties of CO<sub>2</sub> absorption/desorption cycle based on the chemical potential and heat of reaction analysis. According to the pre- and post-combustion technologies and conditions in power-plants, based on our calculated thermodynamic properties of reactions for each solid capturing CO<sub>2</sub>, only those solid materials, which result in lower energy cost in the capture and regeneration process and could work at desired conditions of CO<sub>2</sub> pressure and temperature, will be selected as CO<sub>2</sub> sorbent candidates and further be considered for experimental validation. Compared to experimental thermodynamic data for known systems, our results show that this screening methodology can predict the thermodynamic properties for CO<sub>2</sub> capture sorbents reactions and therefore can be used for screening from vast numbers of solid materials where thermodynamic data are unknown.

In summary, experiments conducted on laboratory-synthesized Na-promoted MgO-based sorbents show high warm CO<sub>2</sub> capture capacity, and appear to be promising CO<sub>2</sub> absorbent in the temperature range of 300~400 °C. The synthesized material precursor mixture is composed of Na<sub>2</sub>Mg(CO<sub>3</sub>)<sub>2</sub>, NaNO<sub>3</sub>, and MgCO<sub>3</sub>·5H<sub>2</sub>O, which after activation converts into sorbent mixture which includes MgO, Na<sub>2</sub>CO<sub>3</sub> and NaNO<sub>3</sub>. The CO<sub>2</sub> absorption process is facilitated through the conversion of MgO and Na<sub>2</sub>CO<sub>3</sub> into Na<sub>2</sub>Mg(CO<sub>3</sub>)<sub>2</sub> double salt with CO<sub>2</sub> exposure. Through the formation of Na-Mg double salt, both the structure stability and reactivity of the sorbent are improved over unmodified MgO. This work has been confirmed by thermodynamics analysis using HSC chemistry package as well as with *ab initio* thermodynamic approach. The major degradation in the capture capacity after the initial absorption is due to the activity loss of the MgO which is derived from MgCO<sub>3</sub>·5H<sub>2</sub>O, while MgO from Na<sub>2</sub>Mg(CO<sub>3</sub>)<sub>2</sub> stays active and contributes to the regenerable CO<sub>2</sub> capacity. Further understanding is needed to improve the absorbent performance and stability.

## Acknowledgement

The authors thank Drs. D. C. Sorescu, G. Richard, B. Li, M. Madhava, J. K. Johnson, B. Zhang, Y. Soong, R. Siriwardane, J. W. Halley and G. Richards for fruitful discussions.

## References

- (1) Aaron, D.; Tsouris, C. *Separation Science and Technology* **2005**, *40*, 321.
- (2) Allen, M. R.; Frame, D. J.; Huntingford, C.; Jones, C. D.; Lowe, J. A.; Meinshausen, M.; Meinshausen, N. *Nature* **2009**, *458*, 1163.
- (3) Haszeldine, R. S. *Science* **2009**, *325*, 1647.
- (4) MacDowell, N.; Florin, N.; Buchard, A.; Hallett, J.; Galindo, A.; Jackson, G.; Adjiman, C. S.; Williams, C. K.; Shah, N.; Fennell, P. *Energy & Environmental Science* **2010**, *3*, 1645.
- (5) Markewitz, P.; Kuckshinrichs, W.; Leitner, W.; Linssen, J.; Zapp, P.; Bongartz, R.; Schreiber, A.; Muller, T. E. *Energy & Environmental Science* **2012**, *5*, 7281.
- (6) White, C. M.; Strazisar, B. R.; Granite, E. J.; Hoffman, J. S.; Pennline, H. W. *Journal of the Air & Waste Management Association* **2003**, *53*, 645.
- (7) Figueroa, J. D.; Fout, T.; Plasynski, S.; McIlvried, H.; Srivastava, R. D. *Int. J. Greenh. Gas Control* **2008**, *2*, 9.
- (8) In [http://www.siemens.com/innovation/en/publikationen/publications\\_pof/pof\\_spring\\_2008/energy/co2\\_speicherung.htm](http://www.siemens.com/innovation/en/publikationen/publications_pof/pof_spring_2008/energy/co2_speicherung.htm)
- (9) Sridhar, N.; Hill, D. [http://www.dnv.com/binaries/dnv-position\\_paper\\_co2\\_utilization\\_tcm4-445820.pdf](http://www.dnv.com/binaries/dnv-position_paper_co2_utilization_tcm4-445820.pdf).

- (10) Rubin, E. S.; Mantripragada, H.; Marks, A.; Versteeg, P.; Kitchin, J. *Progress in Energy and Combustion Science* **2012**, *38*, 630.
- (11) Duan, Y. *Proceedings of 7<sup>th</sup>-10<sup>th</sup> Annual Conference on Carbon Capture and Sequestration 2008-2011*.
- (12) White, C. M.; Strazisar, B. R.; Granite, E. J.; Hoffman, J. S.; Pennline, H. W. *J Air Waste Manag Assoc* **2003**, *53*, 645.
- (13) Abanades, J. C.; Anthony, E. J.; Wang, J.; Oakey, J. E. *Environ. Sci. Technol.* **2005**, *39*, 2861.
- (14) Siriwardane, R.; Poston, J.; Chaudhari, K.; Zinn, A.; Simonyi, T.; Robinson, C. *Energy & Fuels* **2007**, *21*, 1582.
- (15) Siriwardane, R. V.; Stevens, R. W. *Ind. Eng. Chem. Res.* **2009**, *48*, 2135.
- (16) Duan, Y. *Journal of Renewable and Sustainable Energy* **2011**, *3*, 013102.
- (17) Duan, Y. *Journal of Renewable and Sustainable Energy* **2012**, *4*, 013109.
- (18) Duan, Y.; Parlinski, K. *Physical Review B* **2011**, *84*, 104113.
- (19) Duan, Y.; Sorescu, D. C. *Physical Review B* **2009**, *79*, 014301.
- (20) Duan, Y.; Sorescu, D. C. *Journal of Chemical Physics* **2010**, *133*, 074508.
- (21) Duan, Y.; Zhang, B.; Sorescu, D. C.; Johnson, J. K. *J. Solid State Chem.* **2011**, *184*, 304.
- (22) Zhang, B.; Duan, Y.; Johnson, J. K. *Journal of Chemical Physics* **2012**, *136*, 064516.
- (23) Duan, Y.; Luebke, D.; Pennline, H. *International Journal of Clean Coal and Energy* **2012**, *1*, 1.
- (24) Duan, Y. H.; Luebke, D. R.; Pennline, H. W.; Li, B. Y.; Janik, M. J.; Halley, J. W. *Journal of Physical Chemistry C* **2012**, *116*, 14461.
- (25) Duan, Y. H.; Zhang, B.; Sorescu, D. C.; Johnson, J. K.; Majzoub, E. H.; Luebke, D. R. *J. Phys. Condens. Matter* **2012**, *24*.
- (26) Kresse, G.; Hafner, J. *Phys. Rev. B* **1993**, *47*, 558.
- (27) Kresse, G.; Furthmuller, J. *Phys. Rev. B* **1996**, *54*, 11169.
- (28) Perdew, J. P.; Wang, Y. *Physical Review B* **1992**, *45*, 13244.
- (29) Duan, Y. *Phys. Rev. B* **2008**, *77*, 045332.
- (30) Monkhorst, H. J.; Pack, J. D. *Phys. Rev. B* **1976**, *13*, 5188.
- (31) Parlinski, K. *Software PHONON* **2006**.
- (32) Parlinski, K.; Li, Z. Q.; Kawazoe, Y. *Phys. Rev. Lett.* **1997**, *78*, 4063.
- (33) Sternik, M.; Parlinski, K. *J. Chem. Phys.* **2005**, *123*.
- (34) DOE-NETL : "Cost and Performance Baseline for Fossil Energy Plants", Volume 1: Bituminous Coal and Natural Gas to Electricity Final Report; [http://www.netl.doe.gov/energy-analyses/baseline\\_studies.html](http://www.netl.doe.gov/energy-analyses/baseline_studies.html), 2007.
- (35) Mathias, P. M.; Reddy, S.; O'Connell, J. P. *Int. J. Greenh. Gas Control* **2010**, *4*, 174.
- (36) Wang, Q.; Luo, J.; Zhong, Z.; Borgna, A. *Energy & Environmental Science* **2011**, *4*, 42.
- (37) HSC Chemistry software 6.1, Pori: Outotec Research Oy, [www.outotec.com/hsc](http://www.outotec.com/hsc) **2006**.
- (38) Factsage. [www.factsage.com](http://www.factsage.com), 2006-2010.
- (39) Pennline, H. W.; Hoffman, J. S.; Gray, M. L.; Siriwardane, R. V.; Fauth, D. J.; Richards, G. A. NETL in-house postcombustion sorbent-based carbon dioxide capture research. In *Annual NETL CO<sub>2</sub> capture technology for existing plants R&D meeting* Pittsburgh, 2009.
- (40) Hirano, S.; Shigemoto, N.; Yamada, S.; Hayashi, H. *Bull. Chem. Soc. Jpn.* **1995**, *68*, 1030.
- (41) Hayashi, H.; Taniuchi, J.; Furuyashiki, N.; Sugiyama, S.; Hirano, S.; Shigemoto, N.; Nonaka, T. *Ind. Eng. Chem. Res.* **1998**, *37*, 185.
- (42) Lee, S. C.; Kim, J. C. *Catal Surv Asia* **2007**, *11*, 171.
- (43) Shigemoto, N.; Yanagihara, T.; Sugiyama, S.; Hayashi, H. *Energy Fuels* **2006**, *20*, 721.
- (44) Zhao, C. W.; Chen, X. P.; Zhao, C. S.; Liu, Y. K. *Energy Fuels* **2009**, *23*, 1766.
- (45) Essaki, K.; Nakagawa, K.; Kato, M.; Uemoto, H. *J. Chem. Eng. Jpn* **2004**, *37*, 772.
- (46) Kato, M.; Nakagawa, K. *J. Ceram. Soc. Jpn* **2001**, *109*, 911.
- (47) Nakagawa, K.; Ohashi, T. *J. Electrochem. Soc.* **1998**, *145*, 1344.
- (48) Nakagawa, K.; Ohashi, T. *Electrochemistry* **1999**, *67*, 618.
- (49) Olivares-Marin, M.; Drage, T. C.; Maroto-Valer, M. M. *Int. J. Greenh. Gas Control* **2010**, *4*, 623.
- (50) Rodriguez-Mosqueda, R.; Pfeiffer, H. *Journal of Physical Chemistry A* **2010**, *114*, 4535.
- (51) Xiong, R.; Ida, J.; Lin, Y. S. *Chemical Engineering Science* **2003**, *58*, 4377.

- (52) Lopez-Ortiz, A.; Rivera, N. G. P.; Rojas, A. R.; Gutierrez, D. L. *Separation Science and Technology* **2004**, *39*, 3559.
- (53) Zhang, K.; Li, X. S.; Duan, Y.; King, D. L.; Singh, P.; Li, L. *Int. J. Greenh. Gas Control* **2012**, to be submitted.
- (54) Mayorga, S. G.; Weigel, S. J.; Gaffney, T. R.; Brzozowski, J. R. "CARBON DIOXIDE ADSORBENTS CONTAINING MAGNESIUM OXIDE SUITABLE FOR USE AT HIGH TEMPERATURES"; Air Products and Chemical, Inc.: United States, 2001; Vol. US006280503B1; pp 15.
- (55) Gregg, S. J.; Ramsay, J. D. *Journal of the Chemical Society A* **1970**, 2784.
- (56) Bhagiyalakshmi, M.; Lee, J. Y.; Jang, H. T. *Int. J. Greenh. Gas Control* **2010**, *4*, 51.
- (57) Zhang, K.; King, D.; Li, X. S.; Dagle, R.; Li, L.; Duan, Y.; Singh, P. "CARBON CAPTURE-PROMOTED SYNGAS UTILIZATION FOR PRODUCTION OF FUELS AND CHEMICALS"; Proceedings of the 29<sup>th</sup> International Pittsburgh Coal Conference, 2012, Pittsburgh, PA.